

# Holographic model with a NS-NS field

Yunseok Seo<sup>a</sup>, Sang-jin Sin<sup>b</sup> and Wei-shui Xu<sup>a,b</sup>

<sup>a</sup>*Center for Quantum Spacetime, Sogang University, Seoul 121-742, Korea*

<sup>b</sup>*Physics Department, Hanyang University, Seoul 133-791, Korea*

e-mail: *yseo, sjsin@hanyang.ac.kr, wsxuitp@gmail.com*

## Abstract

We consider a holographic model constructed through using the D4/D8- $\overline{D8}$  brane configuration with a NS-NS background field. We study some properties of the effective field theory in this intersecting brane construction, and calculate the effects of this NS-NS background field on some underlying dynamics. We also discuss some other general brane configurations.

# 1 Introduction

The AdS/CFT correspondence proposed by Maldacena is one realization of the holographic principle [1]. It means IIB string theory on the  $AdS_5 \times S^5$  gravity background is dual to the  $\mathcal{N} = 4$  supersymmetric Yang-Mills field theory in the boundary [2]-[5]. In order to use the AdS/CFT method to study more realistic physics, one need to consider some necessary properties, such as less supersymmetries, confinement and chiral symmetry breaking in constructing models. It was firstly given some investigations in the references [4] and [7]. In [8], Karch et al. introduce fundamental flavors into the holographic models by adding some probe flavor D-branes. In the quenching approximation, the supergravity method is a useful way to study some strong coupling dynamics of the boundary field theory. Follow this proposal, many holographic models are constructed to study the strong coupling physics by the supergravity approximation [9]-[14]. If the number of flavor branes is almost equal to the color brane number ( $N_f \sim N_c$ ), it means the flavor backreaction becomes large, then the quenching approximation isn't reliable [15].

Now we generalize to consider the color brane background with a NS-NS  $B_{MN}$  background field. In string theory, we know that a NS-NS  $B_{MN}$  background field produces some non-commutative effects in the field theory on the D-brane world-volume [16], [18] and [19]. The strong and weak coupled regimes of these non-commutative effective field theory can be analyzed as the same way in [20]. After adding the flavor D-brane into such background, one can obtain some non-commutative QCD-like effective field theory on the intersecting region of the brane configuration. Such model was firstly studied in [13]. It is interesting to construct some holographic models with a NS-NS  $B_{MN}$  field from string theory, and investigate some properties of these models by using the gauge/gravity correspondence. Then we can understand such NS-NS  $B_{MN}$  background field how to affect the underlying strong coupled dynamics of the effective field theory.

In this paper, we construct a holographic model through using the brane configuration D4/D8- $\overline{D8}$  just like the Sakai-Sugimoto model [12]. The difference with the Sakai-Sugimoto model is now the color D4-branes gravity background with a NS-NS  $B_{12}$  field (see appendix). If there only exists a constant NS-NS  $B_{12}$  background, then it will be equivalent to turn on a magnetic field on the flavor brane worldvolume by the gauge invariance. But now except for this NS-NS field, the dilaton and R-R field also include this non-commutative parameter  $b$ . Thus, it can't be gauged away by add an additional gauge

field on the flavor brane.

Then the effective field theory on the intersecting region of this brane configuration is four-dimensional and non-commutative along the coordinates  $x_1$  and  $x_2$ . And some strong coupled physics of this effective theory can be studied through investigating the dynamics of the flavor D8-brane in the D4-brane gravity background. If one don't consider the gauge field on the flavor D8-brane, then the effective D8-brane action is same as the commutative case in [12]. The reason is the non-commutative parameter from the dilaton will cancel out with the contribution of the square root part in the D8-brane DBI action. It means that this NS-NS  $B_{12}$  background field doesn't have any effects on the dynamics of the flavor D8-brane. But after a magnetic field along the  $x_1$  and  $x_2$  directions is turned on, then the non-commutative parameter will combine together with this magnetic field, and can't be canceled in the effective D8-brane action. Finally, this effective DBI action contains the contribution of the NS-NS  $B_{12}$  field. And its effects on the chiral symmetry breaking and phase transition etc. can be analyzed in details through using the supergravity/Born-Infeld approximation. We also investigate a fundamental string moving in the near horizon geometry of the black D4-branes. And we calculate the drag force of moving quark and the Regge trajectory of mesons in this non-commutative quark-gluon-plasma(QGP), and analyze the NS-NS  $B_{12}$  how to influence on these quantities.

This papers is organized as follows. In the section 2, we firstly give a brane construction, and study the D8-brane dynamics without and with a magnetic field in the near horizon geometry of the color D4-branes background with a NS-NS  $B_{12}$  field. In the section 3, we generalize to study some other brane configurations by using the same way as in the previous section. Then in the section 4, we study the physics of a fundamental string moving through the near horizon background of the black D4-branes with a NS-NS  $B_{12}$  field. The section 5 is some conclusions and discussions. And finally there is an appendix.

## 2 Brane configuration

We consider a brane configuration which is composed of D4, D8 and  $\overline{\text{D8}}$  brane in IIA string theory. The  $N_c$  D4 are the color branes, while the D8 and  $\overline{\text{D8}}$  branes produce the

flavor degrees of freedom. Their extending directions of these branes are as follows

$$\begin{array}{cccccccccc}
 & 0 & 1 & 2 & 3 & 4 & 5 & 6 & 7 & 8 & 9 \\
 N_c \text{ D4:} & x & x & x & x & x & & & & & \\
 N_f \text{ D8, } \overline{\text{D8}}: & x & x & x & x & & x & x & x & x & x
 \end{array} \tag{2.1}$$

In this brane configuration, the D8 and  $\overline{\text{D8}}$  branes are parallel each other and intersect with the  $N_c$  D4 branes along directions  $(x_0, \dots, x_3)$ . All the others are the transverse directions to the intersection region. We assume the coordinate  $x_4$  to be compactified on a circle  $S^1$ , so it satisfies a periodic condition  $x_4 \sim x_4 + \delta x_4$ . Then the fermions on the D4 brane with anti-periodic boundary condition on this circle get mass and are decoupled from the low energy effective theory. Also we assume the number of the color and flavor branes satisfies the condition  $N_f \ll N_c$ . In this quenching approximation, the backreaction of the flavor branes on the color branes can be ignored. Due to the existence of the NS-NS  $B_{12}$  field, the coordinates  $x_1$  and  $x_2$  are non-commutative

$$[x_1, x_2] \sim b, \tag{2.2}$$

the low energy effective theory in the intersecting region is a non-commutative field theory. If let the non-commutative parameter vanish, the gravity background here reduces to the usual near horizon geometry of D4 branes without a NS-NS background field. So our model correspondingly goes to the Sakai-Sugimoto model [12]. This means that this holographic model is connected to Sakai-Sugimoto model through varying the non-commutative parameter  $b$ . Thus, the holographic model with a NS-NS  $B_{12}$  background field can be regarded as a non-commutative deformation to the Sakai-Sugimoto holographic model.

After compactifying the coordinate  $x_4$  and using the gravity background (A.3) introduced in the appendix, we get the following gravity solution

$$\begin{aligned}
 ds^2 &= \left(\frac{u}{R}\right)^{3/2} [-dt^2 + h(dx_1^2 + dx_2^2) + dx_3^2 + f dx_4^2] + \left(\frac{R}{u}\right)^{3/2} \left(\frac{du^2}{f} + u^2 d\Omega_4^2\right), \\
 R^3 &= \pi^4 g_s N_c, \quad h = \frac{1}{1 + a^3 u^3}, \quad a^3 \equiv \frac{b^2}{R^3}, \quad H = 1 - \frac{u_{KK}^3}{u^3}, \\
 B_{12} &= \frac{a^3 u^3}{b(1 + a^3 u^3)} = \frac{1}{b}(1 - h), \quad e^{2\phi} = \frac{g_s^2 u^{3/2}}{R^{3/2} b^2} h, \\
 C_{01234} &= g_s^{-1} h, \quad C_{034} = g_s^{-1} b.
 \end{aligned} \tag{2.3}$$

In order to avoid the singularity, the coordinate  $x_4$  will be periodic with a radius

$$x_4 \sim x_4 + \delta x_4 = x_4 + \frac{4\pi}{3} \frac{R^{3/2}}{u_{KK}^{1/2}}. \tag{2.4}$$

From this radius of the coordinate  $x_4$ , we know it corresponds to a KK mass scale

$$M_{KK} = \frac{2\pi}{\delta x_4} = \frac{3}{2} \frac{u_{KK}^{1/2}}{R^{3/2}}. \quad (2.5)$$

By using the solution (2.3), and doing a double Wick rotation between the coordinate  $t$  and  $x_4$ , we obtain a black hole solution as follows

$$\begin{aligned} ds^2 &= \left(\frac{u}{R}\right)^{3/2} [-H dt^2 + h(dx_1^2 + dx_2^2) + dx_3^2 + dx_4^2] + \left(\frac{R}{u}\right)^{3/2} \left(\frac{du^2}{H} + u^2 d\Omega_4^2\right), \\ R^3 &= \pi^4 g_s N_c, \quad h = \frac{1}{1 + a^3 u^3}, \quad a^3 \equiv \frac{b^2}{R^3}, \quad H = 1 - \frac{u_H^3}{u^3}, \\ B_{12} &= \frac{a^3 u^3}{b(1 + a^3 u^3)} = \frac{1}{b}(1 - h), \quad e^{2\phi} = \frac{g_s^2 u^{3/2}}{R^{3/2} b^2} h, \\ C_{01234} &= g_s^{-1} h, \quad C_{034} = g_s^{-1} b. \end{aligned} \quad (2.6)$$

Now the coordinates  $t$  and  $x_4$  are all compactified. The time coordinate  $t$  need to be periodic

$$t \sim t + \delta t = t + \frac{4\pi}{3} \frac{R^{3/2}}{u_H^{1/2}}, \quad (2.7)$$

then this background is well-defined. And the corresponding temperature of this black hole is

$$T = \frac{3}{4\pi} \frac{u_H^{1/2}}{R^{3/2}}. \quad (2.8)$$

Through a Hawking-Page phase transition at a critical point  $u_H = u_{KK}$ , the low temperature solution (2.3) will go to the black hole background (2.6).

## 2.1 Low temperature phase

For the low temperature phase, the dominated gravity background is the equation (2.3). Now we consider the dynamics of the probe D8- $\overline{\text{D8}}$  brane in this background. Assume the transverse coordinate  $x_4$  of D8 branes is a function of the radial coordinate  $u$ , i.e.  $x_4 = x_4(u)$ . Then the induced metric on the D8 branes is

$$\begin{aligned} ds^2 &= \left(\frac{u}{R}\right)^{3/2} [-dt^2 + h(dx_1^2 + dx_2^2) + dx_3^2] + \left(\frac{R}{u}\right)^{3/2} u^2 d\Omega_4^2 \\ &\quad + \left[ \left(\frac{R}{u}\right)^{3/2} f^{-1} + f \left(\frac{u}{R}\right)^{3/2} \left(\frac{\partial x_4}{\partial u}\right)^2 \right] du^2, \end{aligned} \quad (2.9)$$

Using the D-brane effective action

$$S = S_{DBI} + S_{CS},$$

$$\begin{aligned}
S_{DBI} &= -T_p \int d^{p+1} \xi e^{-\phi} \sqrt{-\det(P[G + B]_{\mu\nu} + 2\pi F_{\mu\nu})}, \\
S_{CS} &= T_p \int \sum_i P[C_i \wedge e^{B_2}] \wedge e^{2\pi F_2},
\end{aligned} \tag{2.10}$$

then we get the D8-brane action is <sup>1</sup>

$$S_{DBI} \sim \int du u^{13/4} \sqrt{\left(\frac{R}{u}\right)^{3/2} f^{-1} + f \left(\frac{u}{R}\right)^{3/2} \left(\frac{\partial x_4}{\partial u}\right)^2}, \tag{2.11}$$

and

$$S_{CS} = 0. \tag{2.12}$$

Except for the proportional coefficient, this action is same as the D8-brane effective in the D4-branes background without a NS-NS  $B_{12}$  background field. The reason is the  $h$  included in the term  $e^{-\phi}$  will be canceled out with the same factor in the square root part of the DBI action. Thus, at low temperature, the NS-NS background field doesn't influence on the dynamics of the probe D8-brane in this non-commutative gravity background. Its dynamics is same with the usual commutative case [12] and [21].

Then one can get two different solutions from the equation of motion: one is the connected configuration of the D8- $\overline{\text{D8}}$  branes, the other is the separated case. The connected solution corresponds to the chiral symmetry breaking phase, while the chiral symmetry is preserved for the separated solution. But the on-shell energy difference between the connected and separated solution is always negative, so this connected configuration is dominated in the low temperature phase [21]. The chiral symmetry is always broken  $U(N_f) \times U(N_f) \rightarrow U(N_f)_{\text{diag}}$ , and the corresponding Nambu-Goldstone boson can be found through calculating the meson spectra [12].

## 2.2 High temperature phase

In the high temperature phase, the corresponding gravity background is the black solution (2.6). We still assume the transverse coordinate  $x_4$  of the flavor D8-brane depends on the coordinate  $u$ , then the induced metric on the D8-brane is

$$ds^2 = \left(\frac{u}{R}\right)^{3/2} [-H dt^2 + h(dx_1^2 + dx_2^2) + dx_3^2]$$

---

<sup>1</sup>Here we don't turn on the gauge field on the D8 brane worldvolume, so to investigate the dynamics of D8-brane in the gravity background (2.3), it is enough to only use the effective action of one single flavor D8 brane.

$$+ \left( \left( \frac{R}{u} \right)^{3/2} H^{-1} + \left( \frac{u}{R} \right)^{3/2} \left( \frac{\partial x_4}{\partial u} \right)^2 \right) du^2 + \left( \frac{R}{u} \right)^{3/2} u^2 d\Omega_4^2. \quad (2.13)$$

So the effective action of the D8-brane is

$$S \sim \int du u^{13/4} H^{1/2} \sqrt{\left( \frac{R}{u} \right)^{3/2} H^{-1} + \left( \frac{u}{R} \right)^{3/2} \left( \frac{\partial x_4}{\partial u} \right)^2}. \quad (2.14)$$

Clearly, it still doesn't depend on the NS-NS background field, and is also same as the commutative case [12] except for the proportional coefficient. Then all the other analysis of the D8- $\overline{\text{D8}}$  dynamics will be same. Through comparing the energy of these two solutions, one can find there exists two phase at high temperature. One is the chiral symmetry breaking phase, the other is chiral symmetry restoration phase. Between these two phases, it has a chiral phase transition at a critical temperature. Below this critical temperature the system is located at the chiral symmetry breaking phase i.e.  $U(N_f) \times U(N_f) \rightarrow U(N_f)_{\text{diag}}$ , otherwise it will be in the chiral symmetry restoration phase.

### 2.3 Adding a magnetic field

Now we introduce a constant magnetic field along the  $x_1$  and  $x_2$  directions

$$2\pi F_{12} = B, \quad (2.15)$$

on the flavor D8-brane<sup>2</sup>. This magnetic field is equivalent to a constant NS-NS  $B'_{12}$  field by the gauge invariance on the D8-brane. This NS-NS  $B'_{12}$  field will contribute a constant transportation to the NS-NS  $B_{12}$  field

$$B_{\text{new}} = B_{12} + B'_{12} = B + \frac{1 - h(u)}{b}. \quad (2.16)$$

This new background is still a solution of the IIA supergravity. Since the dilation and R-R field in the gravity background all depend on the parameter  $b$ , this magnetic field  $B$  can't be canceled out through a redefinition of the parameter  $b$ . Then the flavor D8-brane effective action contains the contributions of the NS-NS  $B_{12}$  and magnetic field together. In the following we will analyze the effect of the parameters  $b$  and  $B$  on the flavor brane dynamics in details.

---

<sup>2</sup> Holographic models with a constant magnetic or electric field were studied in [22]-[25].

### 2.3.1 Low temperature

The induced metric on the flavor D8-brane is same as the equation (2.9). After a magnetic field (2.15) is turned on, the effective action of the probe D8 brane is

$$S \sim \int du \frac{u^{7/4}}{\sqrt{h}} \sqrt{A(u)} \sqrt{\left(\frac{R}{u}\right)^{3/2} f^{-1} + \left(\frac{u}{R}\right)^{3/2} f \left(\frac{\partial x_4}{\partial u}\right)^2}, \quad (2.17)$$

where the  $A(u)$  is defined as

$$A(u) \equiv \frac{u^3}{R^3 + b^2 u^3} + \frac{B^2}{1 + 2bB}. \quad (2.18)$$

It is clear that the factor  $A(u)$  can't be canceled each other with the  $h(u)$  in the action (2.17) through introducing this magnetic field. If the magnetic field vanishes  $B = 0$ , then this effective action will reduce to the action (2.11).

Now the equation of motion from the action (2.17) is

$$\frac{\partial}{\partial x_4} \left[ \frac{u^{5/2}}{\sqrt{h}} \frac{f \sqrt{A(u)}}{\sqrt{f + f^{-1} \left(\frac{R}{u}\right)^3 u'^2}} \right] = 0. \quad (2.19)$$

Choose a boundary condition  $u' = 0$  at  $u = u_0$  and perform an integration<sup>3</sup>, we get a first derivative equation

$$\frac{u^{5/2}}{\sqrt{h}} \frac{f \sqrt{A(u)}}{\sqrt{f + f^{-1} \left(\frac{u}{R}\right)^3 u'^2}} = \frac{u_0^{5/2} \sqrt{f(u_0) A(u_0)}}{\sqrt{h(u_0)}}. \quad (2.20)$$

Then the  $u'$  equation is

$$u' = \sqrt{P(u)}, \quad P(u) \equiv \left(\frac{u}{R}\right)^3 f^2 \left[ \left(\frac{u}{u_0}\right)^5 \frac{h(u_0) A(u) f(u)}{h(u) A(u_0) f(u_0)} - 1 \right]. \quad (2.21)$$

Defining  $y \equiv \frac{u}{u_0}$ ,  $y_{KK} \equiv \frac{u_{KK}}{u_0}$  and  $z = y^{-3}$ , we can rewrite the above equation  $P(u)$  as

$$\begin{aligned} P &= \frac{u_0^3}{R^3} y^3 f(y)^2 \left[ y^5 \frac{h(1) A(y) f(y)}{h(y) A(1) f(1)} - 1 \right] \\ &= \frac{u_0^3}{R^3} z^{-1} f(z)^2 \left[ z^{-5/3} \frac{h(1) A(z) f(z)}{h(z) A(1) f(1)} - 1 \right]. \end{aligned} \quad (2.22)$$

---

<sup>3</sup>Here the  $'$  denotes  $\partial_{x_4}$ .

So the shape of this connected D8- $\overline{\text{D8}}$  brane solution is

$$x_4(u) = \int_{u_0}^u \frac{du}{\sqrt{P(u)}}. \quad (2.23)$$

The corresponding chiral symmetry in the effective field theory is broken because of this connected solution. Then the asymptotic distance between the D8 and  $\overline{\text{D8}}$  reads

$$L = 2 \int_{u_0}^{\infty} \frac{du}{\sqrt{P(u)}} = \frac{2u_0}{3} \int_0^1 \frac{dz}{z^{4/3} \sqrt{P(z)}}. \quad (2.24)$$

We plot some figures 1-3 to show this asymptotic distance how to depend on the variable  $b$ ,  $B$  and  $y_{KK}$  in this low temperature phase<sup>4</sup>. These figures shows the asymptotic

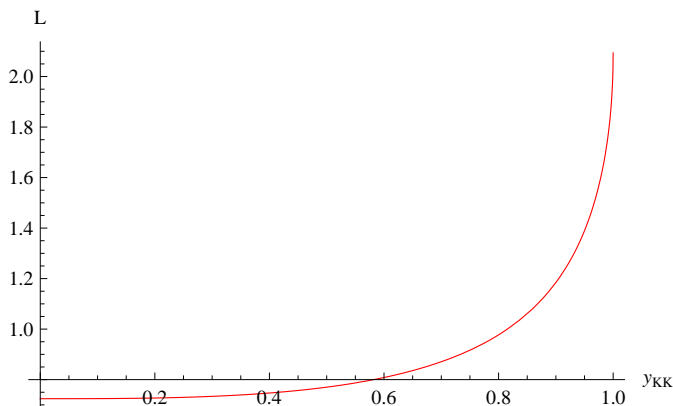


Figure 1: The asymptotic distance  $L$  between the D8 and  $\overline{\text{D8}}$  varies with  $y_{KK}$  at  $b$ ,  $B = 0$ .

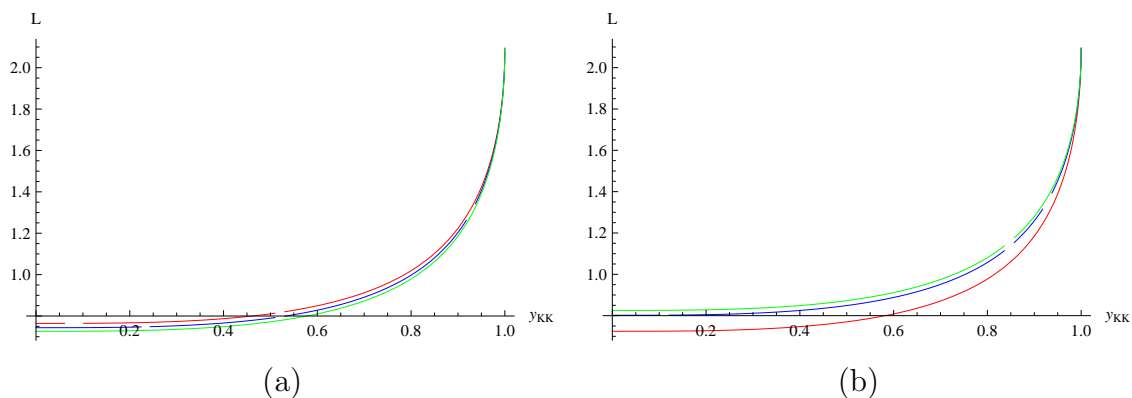


Figure 2: The asymptotic distance  $L$ : (a)  $b = 1, 2, 9$  (red, blue, green) or (from top to bottom) and  $B = 1$ ; (b)  $B = 0, 3, 9$  (red, blue, green) or (from bottom to top) and  $b = 1$ .

<sup>4</sup>In this section, we always choose  $R = u_0 = 1$  in doing the numerical calculations.

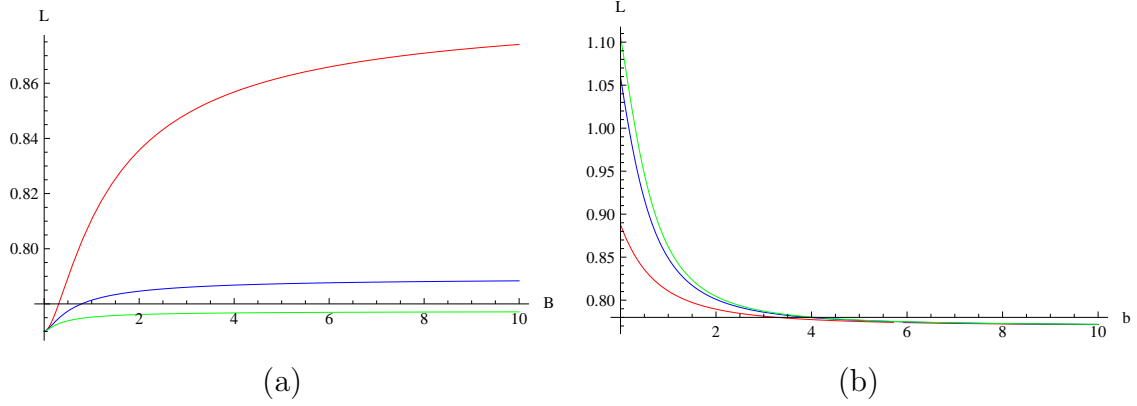


Figure 3: The asymptotic distance  $L$ : (a)  $b = 1, 3, 5$  (red, blue, green) or (from top to bottom) and  $y_{KK} = 0.5$ ; (b)  $B = 1, 3, 5$  (red, blue, green) or (from bottom to top) and  $y_{KK} = 1$ .

distance  $L$  between the D8 and  $\overline{\text{D8}}$  brane is became larger with increasing the value  $y_{KK}$  at arbitrary value  $b$  and  $B$ . For a fixed  $B$  and increasing  $b$ , then  $L$  is decreased. However, for a fixed  $b$  and increasing  $B$ , the distance  $L$  is also increased. So the magnetic field  $B$  and non-commutative parameter  $b$  have a converse contribution to the asymptotic distance  $L$ .

Substituting the equation of motion (2.20) into the effective action (2.17), we obtain the on-shell energy of this connected D8- $\overline{\text{D8}}$  configuration

$$S_{connected} \sim \int_{u_0}^{\infty} du \frac{u^{7/4} \sqrt{A(u)}}{\sqrt{h}} \sqrt{\left(\frac{R}{u}\right)^{3/2} f^{-1} + f \left(\frac{u}{R}\right)^{3/2} \frac{1}{P(u)}}. \quad (2.25)$$

And the energy of the separated D8- $\overline{\text{D8}}$  brane solution  $\partial_u x_4 = 0$  is

$$S_{separated} \sim \int_{u_{KK}}^{\infty} du \frac{R^{3/4} u \sqrt{A(u)}}{\sqrt{h(u) f(u)}}. \quad (2.26)$$

Then the energy difference of these two solutions is

$$\begin{aligned} \delta S &= S_{connected} - S_{separated} \\ &\sim \int_{u_0}^{\infty} du \frac{u \sqrt{A(u)}}{\sqrt{h(u)}} \left( \sqrt{f^{-1} + f \left(\frac{u}{R}\right)^3 \frac{1}{P(u)}} - f^{-1/2} \right) \\ &\quad - \int_{u_{KK}}^{u_0} du \frac{u \sqrt{A(u)}}{\sqrt{h(u) f(u)}} \\ &\sim \frac{1}{3} \int_0^1 dz \frac{\sqrt{A(z)}}{z^{5/3} \sqrt{h}} \left( \sqrt{f(z)^{-1} + \left(\frac{u_0}{R}\right)^3 \frac{f(z)}{P(z)} z^{-1}} - f(z)^{-1/2} \right) \\ &\quad - \int_{y_{KK}}^1 dy \frac{y \sqrt{A(y)}}{\sqrt{h(y) f(y)}}. \end{aligned} \quad (2.27)$$

In the figures 4 and 5, it shows this energy difference varying with the parameter  $B$ ,  $b$  and  $y_{KK}$ . We find the contribution of the parameters  $B$  and  $b$  are similar to the

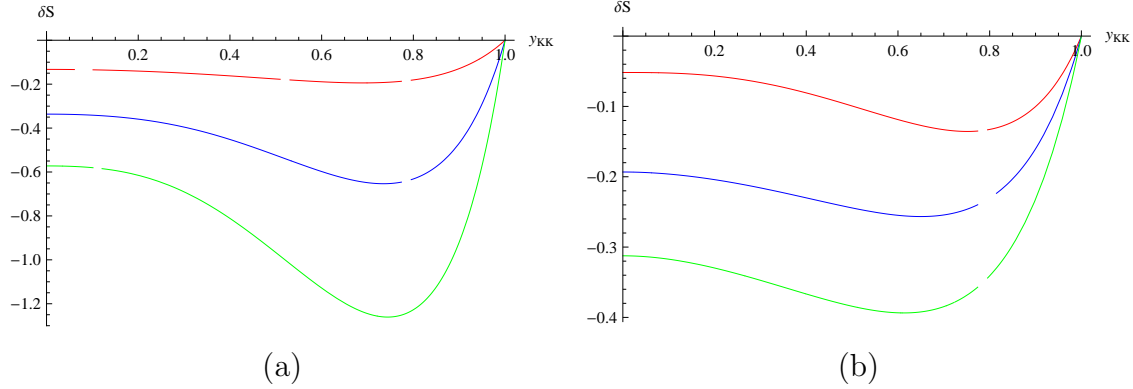


Figure 4: The energy difference  $\delta S$ : (a)  $b = 1, 3, 5$  (red, blue, green) or (from top to bottom) and  $B = 1$ ; (b)  $B = 0, 2, 5$  (red, blue, green) or (from top to bottom) and  $b = 1$ .

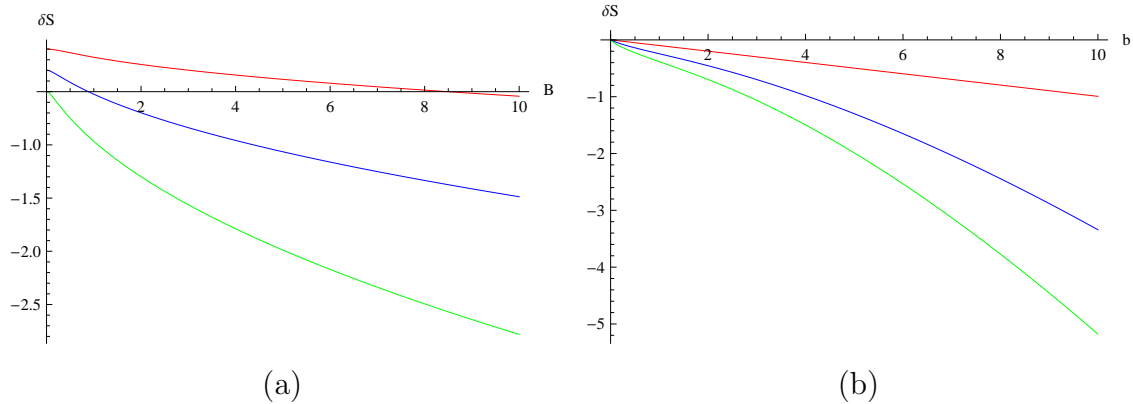


Figure 5: The energy difference  $\delta S$ : (a)  $b = 1, 3, 5$  (red, blue, green) or (from top to bottom) and  $y_{KK} = 0.5$ ; (b)  $B = 0, 2, 5$  (red, blue, green) or (from top to bottom) and  $y_{KK} = 0.5$ .

energy difference  $\delta S$ . And this energy difference is always negative at arbitrary values of the parameters  $b$ ,  $B$  and  $y_{KK}$ . So the connected  $D8-\overline{D8}$  brane configuration is always dominated, and the chiral symmetry of the effective non-commutative field theory is always broken in the low temperature.

### 2.3.2 High temperature

If the magnetic field (2.15) is included, the effective D8 brane action in the black hole background (2.6) is

$$S \sim \int du \frac{u^{7/4} \sqrt{A}}{\sqrt{h}} \sqrt{\left(\frac{R}{u}\right)^{3/2} + H(u) \left(\frac{u}{R}\right)^{3/2} \left(\frac{\partial x_4}{\partial u}\right)^2}. \quad (2.28)$$

Now the effective action contains the parameters  $B$  and  $b$  through the factor  $A(u)$  and  $h(u)$ . Since the action (2.28) doesn't explicitly depend on the coordinate  $x_4$ , the Hamiltonian relative to the variable  $x_4$  is conserved. So the equation of motion is

$$\frac{\partial}{\partial x_4} \left[ \frac{u^{5/2} H \sqrt{A(u)}}{\sqrt{h(u) \left(H + \left(\frac{R}{u}\right)^3 u'^2\right)}} \right] = 0. \quad (2.29)$$

As the same way used at low temperature, we choose a boundary condition as  $u' = 0$  at  $u = u_0$ , it corresponds to the connected D8- $\overline{\text{D8}}$  brane solution. Then we obtain a first derivative equation

$$\frac{u^{5/2} H \sqrt{A}}{\sqrt{h \left(H + \left(\frac{R}{u}\right)^3 u'^2\right)}} = \frac{u_0^{5/2} \sqrt{H(u_0) A(u_0)}}{\sqrt{h(u_0)}}. \quad (2.30)$$

In the new variables  $y \equiv \frac{u}{u_0}$  and  $z \equiv y^{-3}$ , the equation can be written as

$$\begin{aligned} u' &= \sqrt{Q(u)}, \\ Q(u) &\equiv \left(\frac{u}{R}\right)^3 \left( \frac{u^5 H(u)^2 A(u) h(u_0)}{h(u) A(u_0) H(u_0) u_0^5} - H(u) \right) \\ &= \frac{u_0^3}{R^3} z^{-1} \left( \frac{H(z)^2 A(z) h(1)}{z^{5/3} h(z) A(1) H(1)} - H(z) \right). \end{aligned} \quad (2.31)$$

So the asymptotic distance between the D8 and  $\overline{\text{D8}}$  defines

$$L = 2 \int_{u_0}^{\infty} \frac{du}{\sqrt{Q(u)}} = \frac{2u_0}{3} \int_0^1 \frac{dz}{z^{4/3} \sqrt{Q(z)}}. \quad (2.32)$$

Through some numerical calculations, we plot figures 6, 7 and 8 about this asymptotic distance  $L$  varying with the parameter  $b$ ,  $B$  and  $y_H$ . The asymptotic distance  $L$  of the D8 and  $\overline{\text{D8}}$  brane become larger with increasing the value  $B$  and a fixed value  $b$ . However, for a fixed  $B$ , then  $L$  is decreased with increasing the value  $b$ . As at low temperature, the

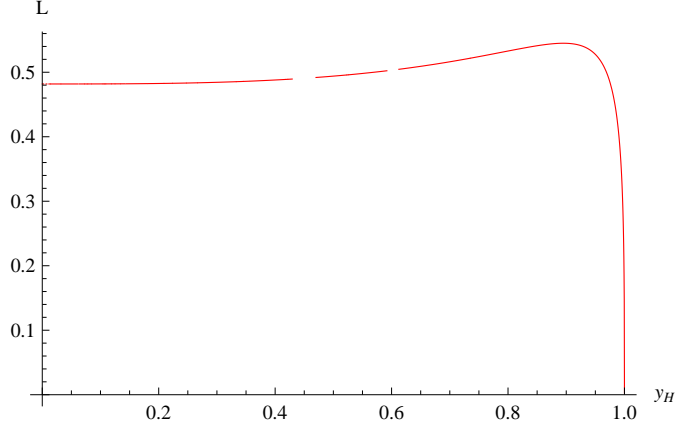


Figure 6: The asymptotic distance  $L$  is shown at  $b$ ,  $B = 0$ .

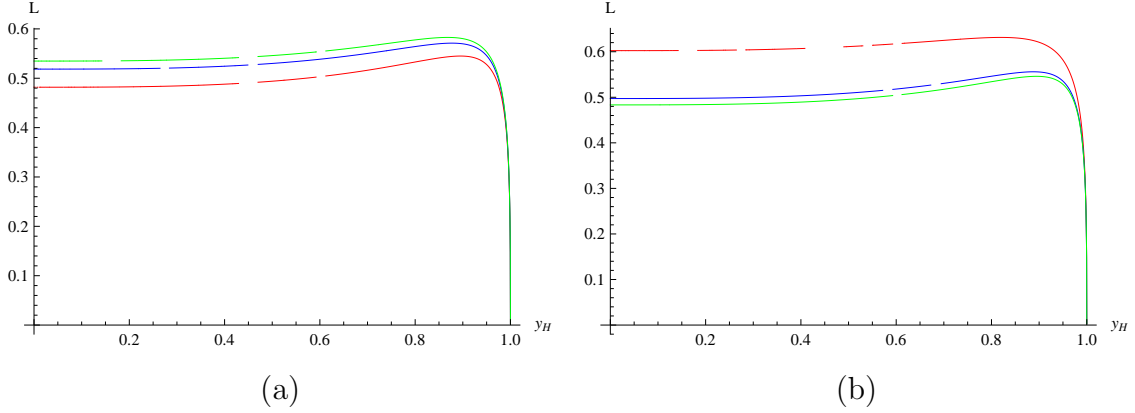


Figure 7: The asymptotic distance  $L$ : (a)  $B = 0, 2, 6$  (red, blue, green) or (from bottom to top) and  $b = 1$ ; (b)  $b = 0, 2, 8$  (red, blue, green) (from top to bottom) and  $B = 2$ .

magnetic parameter  $B$  and non-commutative parameter  $b$  have a converse contribution to the asymptotic distance  $L$  between D8 and  $\overline{\text{D8}}$ .

For this connected D8- $\overline{\text{D8}}$  brane solution, after inserting the solution into the effective action (2.28), we obtain its on-shell energy

$$S_{connected} \sim \int_{u_0}^{\infty} \frac{u^{7/4} A(u)}{\sqrt{h(u)}} \sqrt{\left(\frac{R}{u}\right)^{3/2} + \left(\frac{u}{R}\right)^{3/2} \frac{H(u)}{Q(u)}}. \quad (2.33)$$

Similar as the low temperature case, there also exists a separated D8- $\overline{\text{D8}}$  solution, and its energy is

$$S_{separated} \sim \int_{u_H}^{\infty} du \frac{u^{7/4} A(u)}{\sqrt{h(u)}} \left(\frac{R}{u}\right)^{3/4}. \quad (2.34)$$

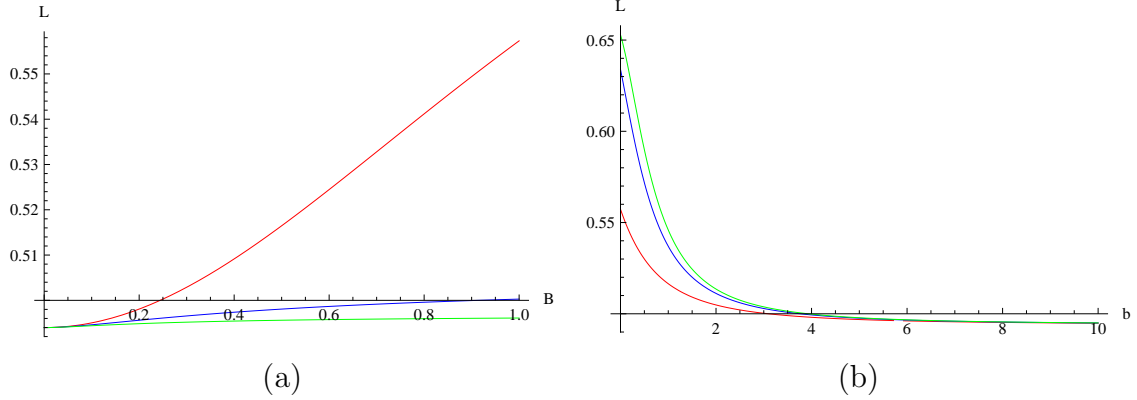


Figure 8: The asymptotic distance  $L$ : (a)  $b = 0, 3, 6$  (red, blue, green) or (from top to bottom) and  $y_H = 0.5$ ; (b)  $B = 1, 3, 6$  (red, blue, green) or (from bottom to top) and  $y_H = 0.5$ .

So the difference of the energy is

$$\begin{aligned}
\delta S &= S_{connected} - S_{separated} \\
&\sim \int_{u_0}^{\infty} du \frac{u\sqrt{A(u)}}{\sqrt{h(u)}} \left( \sqrt{1 + \left(\frac{u}{R}\right)^3 \frac{H(u)}{Q(u)}} - 1 \right) \\
&\quad - \int_{u_H}^{u_0} du \frac{u\sqrt{A(u)}}{\sqrt{h(u)}} \\
&\sim \frac{1}{3} \int_0^1 dz \frac{\sqrt{A(z)}}{z^{5/3}\sqrt{h(z)}} \left( \sqrt{1 + \frac{u_0^3}{R^3} \frac{H(z)}{Q(z)} z^{-1}} - 1 \right) \\
&\quad - \int_{y_H}^1 dy \frac{y\sqrt{A(y)}}{\sqrt{h(y)}}. \tag{2.35}
\end{aligned}$$

We explicitly show this energy difference  $\delta S$  in the figures 9 and 10.

It is clear that the energy difference between the connected and separated solutions has critical point  $y_H^c$ , i.e. critical temperature  $T_\xi$ . If  $B = b = 0$ , this holographic model becomes the Sakai-Sugimoto model. This chiral phase transition is studied in [21]. At  $b = 0$  and a finite  $B$ , the chiral phase transition is also investigated in [24]. The results got here at  $B = b = 0$  or  $b = 0$  is all same as in [21] and [24]. At a fixed value  $b$ , the critical point value  $y_H$  becomes smaller with increasing the value  $B$  in figure 10(a). However, it become larger with increasing the value  $b$  for a fixed  $B$  in figure 10(b). The influences of the parameters  $B$  and  $b$  is very little. Just like the effects on the asymptotic distance, these two parameters also have converse contributions to the critical point of phase transition.

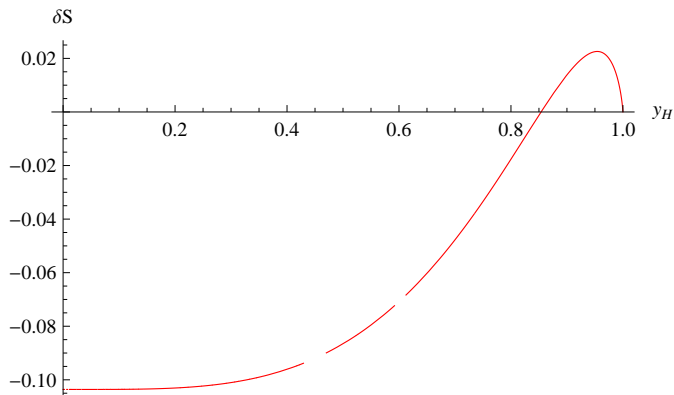


Figure 9: This figure is the energy difference  $\delta S$  at  $B = 0$  and  $b = 0$ .

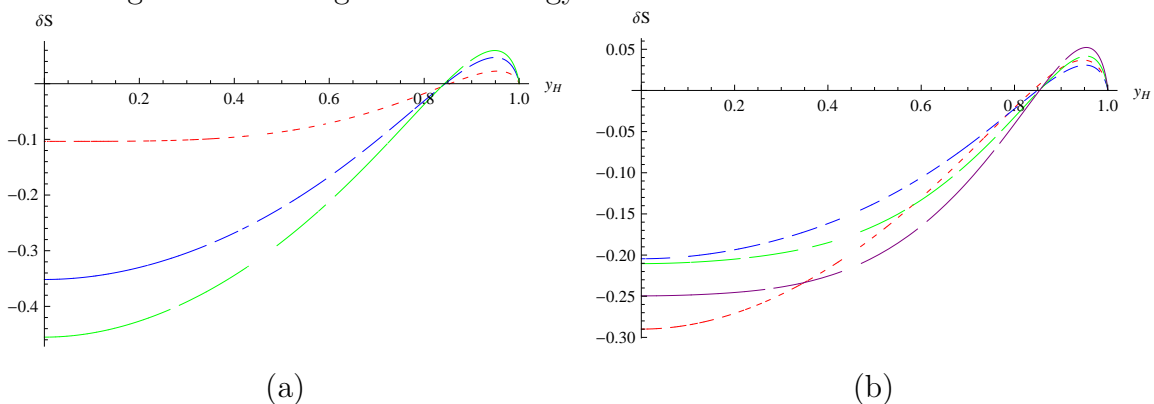


Figure 10: It is the energy difference  $\delta S$ : (a) at  $B = 0, 2, 5$  (red, blue, and green) or (the length of the dashed line segment is increased) and  $b = 1$ ; (b) at  $b = 0, 1, 5, 9$  (red, blue, green and purple) or (the length of the dashed line segment becomes larger) and  $B = 1$ .

Below these critical points, the energy difference  $\delta S$  is negative, otherwise, it become positive. It means there exists two phases at high temperature. The phase transition is first-order between each other. Under the value  $y_H^c$ , the connected solution is dominated, then the chiral symmetry in the four-dimensional field theory will be broken  $U(N_f) \times U(N_f) \rightarrow U(N_f)_{\text{diag}}$ . Otherwise, the dominated solution is the separated D8- $\overline{\text{D8}}$  configuration, and the chiral symmetry will be restored.

### 3 General brane configuration

In this section, we generalize to consider some other brane configurations. Here we mainly consider the color brane still is the D4-branes, so the corresponding gravity backgrounds are the equations (2.3) and (2.6).

Firstly, let us consider the following brane constructions

$$\begin{array}{cccccccccc}
& 0 & 1 & 2 & 3 & 4 & 5 & 6 & 7 & 8 & 9 \\
N_c \text{ D4} : & \text{x} & \text{x} & \text{x} & \text{x} & \text{x} & & & & & \\
N_f \text{ D6, } \overline{\text{D6}} : & \text{x} & \text{x} & \text{x} & \text{x} & & \text{x} & \text{x} & \text{x} & & \\
N_f \text{ D4, } \overline{\text{D4}} : & \text{x} & \text{x} & \text{x} & \text{x} & & \text{x} & & & & 
\end{array} \tag{3.1}$$

The effective field theory on the intersecting region is some four-dimensional non-commutative theory. Follow the same method in the previous subsection, we can analyze the dynamics of these non-commutative field theory at strong coupled regime by supergravity approximation. The effective action of the flavor brane in the low temperature background (2.3) and black hole background (2.6) are as follows

$$S_{\text{low}} \sim \int duu^n \sqrt{\left(\frac{R}{u}\right)^{3/2} f^{-1} + \left(\frac{u}{R}\right)^{3/2} \left(\frac{\partial x_4}{\partial u}\right)^2}, \tag{3.2}$$

$$S_{\text{High}} \sim \int duu^n \sqrt{\left(\frac{R}{u}\right)^{3/2} + H(u) \left(\frac{u}{R}\right)^{3/2} \left(\frac{\partial x_4}{\partial u}\right)^2}. \tag{3.3}$$

For the flavor D6-brane, the parameter  $n$  is  $11/4$ , while  $n = 9/4$  for the D4-brane. The non-commutative parameter  $b$  is canceled in the effective action. So the classical dynamics of flavor brane is same as the commutative cases. At low temperature, the chiral symmetry is always broken. However, there exists a chiral phase transition in the high temperature phase. Below a critical temperature, the chiral symmetry is broken, it corresponds to the connected D8- $\overline{\text{D8}}$  brane solution. Otherwise, the solution is a separated brane configuration, and this symmetry is restored.

Also some three-dimensional non-commutative effective field theories can be constructed through the following brane configurations

$$\begin{array}{cccccccccc}
& 0 & 1 & 2 & 3 & 4 & 5 & 6 & 7 & 8 & 9 \\
N_c \text{ D4} : & \text{x} & \text{x} & \text{x} & \text{x} & \text{x} & & & & & \\
N_f \text{ D6, } \overline{\text{D6}} : & \text{x} & \text{x} & \text{x} & & & \text{x} & \text{x} & \text{x} & \text{x} & \\
N_f \text{ D4, } \overline{\text{D4}} : & \text{x} & \text{x} & \text{x} & & & \text{x} & \text{x} & & & 
\end{array} \tag{3.4}$$

Now the flavor D6 and D4-brane effective actions at low and high temperature background read

$$S_{\text{low}} \sim \int duu^m \sqrt{\left(\frac{R}{u}\right)^{3/2} f^{-1} + \left(\frac{u}{R}\right)^{3/2} \left(\frac{\partial x_4}{\partial u}\right)^2}, \tag{3.5}$$

$$S_{\text{high}} \sim \int duu^m \sqrt{\left(\frac{R}{u}\right)^{3/2} + H(u) \left(\frac{u}{R}\right)^{3/2} \left(\frac{\partial x_4}{\partial u}\right)^2}, \tag{3.6}$$

where the parameter  $m$  is equal to  $9/4$  for the D6-brane, and is  $7/4$  for the D4-brane. Again these effective action are same as the commutative cases.

As the same discussions in the above subsections, one can turn on a magnetic field along the directions  $x_1$  and  $x_2$  on the worldvolume of the flavor branes. Then in the flavor D-brane effective action there will exist some contributions of the  $B$  and  $b$  through  $A(u)$  and  $h(u)$ . Here we list these effective actions: (a) for brane configurations (3.1), the corresponding effective actions are

$$S_{\text{low}_{\text{bB}}} \sim \int du \frac{u^{n-3/2}}{\sqrt{h(u)}} \sqrt{A(u)} \sqrt{\left(\frac{R}{u}\right)^{3/2} f^{-1} + \left(\frac{u}{R}\right)^{3/2} \left(\frac{\partial x_4}{\partial u}\right)^2}, \quad (3.7)$$

$$S_{\text{High}_{\text{bB}}} \sim \int du \frac{u^{n-3/2}}{\sqrt{h(u)}} \sqrt{A(u)} \sqrt{\left(\frac{R}{u}\right)^{3/2} + H(u) \left(\frac{u}{R}\right)^{3/2} \left(\frac{\partial x_4}{\partial u}\right)^2}; \quad (3.8)$$

(b) for brane configurations (3.4), the actions read

$$S_{\text{low}_{\text{bB}}} \sim \int du \frac{u^{m-3/2}}{\sqrt{h(u)}} \sqrt{A(u)} \sqrt{\left(\frac{R}{u}\right)^{3/2} f^{-1} + \left(\frac{u}{R}\right)^{3/2} \left(\frac{\partial x_4}{\partial u}\right)^2}, \quad (3.9)$$

$$S_{\text{high}_{\text{bB}}} \sim \int du \frac{u^{m-3/2}}{\sqrt{h(u)}} \sqrt{A(u)} \sqrt{\left(\frac{R}{u}\right)^{3/2} + H(u) \left(\frac{u}{R}\right)^{3/2} \left(\frac{\partial x_4}{\partial u}\right)^2}. \quad (3.10)$$

Then we can investigate some effects of the NS-NS  $B_{12}$  and magnetic field  $B$  on the string coupled dynamics of the non-commutative effective field theory through using gauge/gravity correspondence. One will find some similar results as the previous subsection. And maybe these holographic models can be used to study some condensed matter physics, for example the quantum Hall effect [36].

Also we can generalize to consider some other color brane background with a NS-NS field, and construct the general Dq/Dp- $\overline{\text{Dp}}$  brane configurations. Then one can study some influences of this NS-NS background field on some properties of the effective theories living on the intersecting parts of these brane configurations by the AdS/CFT correspondence.

## 4 String in non-commutative background

In this section, we consider the dynamics of a fundamental string in the high temperature phase. We calculate the drag force of a quark moving through the QGP, and also study the Regge trajectory of a meson in this non-commutative QGP.

## 4.1 Quark in non-commutative QGP

The Nambu-Goto action of a fundamental string is

$$S = -\frac{1}{2\pi\alpha'} \int d\tau d\sigma \sqrt{-\det g_{\alpha\beta}} + \frac{1}{2\pi\alpha'} \int P[B], \quad g_{\alpha\beta} \equiv \partial_\alpha X^\mu \partial_\beta X^\nu G_{\mu\nu}. \quad (4.1)$$

We consider the two endpoints of a fundamental string separately attached on the black horizon and flavor D8-brane. Following the same way in [26] and [27], we parameterize the world-sheet coordinates of this fundamental string as  $\tau = t$  and  $\sigma = u$ , and assume the endpoint (quark) on the flavor brane moving along the direction  $x_2$  with

$$x_2 = vt + \xi(u). \quad (4.2)$$

Since there exists a rotational symmetry in the  $x_1$  and  $x_2$  plane, it is equivalent to let quark moving along the direction  $x_1$ .

So the induced metric on the string worldsheet is

$$\begin{aligned} g_{\tau\tau} &= -\left(\frac{u}{R}\right)^{3/2} (H - hv^2), \quad g_{\tau\sigma} = g_{\sigma\tau} = \left(\frac{u}{R}\right)^{3/2} hv\xi', \\ g_{\sigma\sigma} &= \left(\frac{u}{R}\right)^{3/2} h\xi'^2 + \left(\frac{R}{u}\right)^{3/2} H^{-1}, \end{aligned} \quad (4.3)$$

where the  $'$  denotes  $\partial_u$ . Then inserting it into the string action, we get

$$\begin{aligned} S &= -\frac{1}{2\pi\alpha'} \int dt du \mathcal{L}, \\ \mathcal{L} &\equiv \sqrt{1 - hH^{-1}v^2 + \left(\frac{u}{R}\right)^3 hH\xi'^2}. \end{aligned} \quad (4.4)$$

The NS-NS  $B_{12}$  field is a two-form along the directions  $x_1$  and  $x_2$ . Since in the coordinate parameterizations the coordinate  $x_1$  is independent of the string world-sheet coordinates  $\tau$  and  $\sigma$ , this NS-NS field doesn't have any contributions to the string action. The string world-sheet momentum of string world-sheet is defined as

$$P_{x_2}^r = \frac{\partial \mathcal{L}}{\partial(\partial_r x_2)} = \Pi_\xi, \quad (4.5)$$

where the canonical momentum is  $\Pi_\xi = \partial_{\xi'} L$ . The string momentum is the energy associated by the fundamental string. So the drag force is

$$-f = \frac{1}{2\pi\alpha'} \Pi_\xi. \quad (4.6)$$

Since the string action (4.4) doesn't explicitly depend on the variable  $\xi$ , the canonical momentum  $\Pi_\xi$  is conserved relative to the parameter  $\xi$ . Then the equation of motion is derived as

$$\xi' = \pm \Pi_\xi \left( \frac{R}{u} \right)^{3/2} \sqrt{\frac{1 - hH^{-1}v^2}{\left(\frac{u}{R}\right)^3 h^2 H^2 - hH\Pi_\xi^2}}. \quad (4.7)$$

Here we need to choose "+" equation because the fundamental string is received a drag force. The  $h(u)$  is positive, and  $H(u)$  is 0 at the horizon and is equal to 1 at infinity. So to preserve the quantity to be positive in the square root in the equation (4.7), the canonical momentum need to satisfy

$$\Pi_\xi = \left( \frac{u_c}{R} \right)^{3/2} h(u_c)v, \quad (4.8)$$

where the coordinate  $u_c$  is chosen as

$$u_c^3 = \frac{1}{2a^3} \left( -(1 - a^3 u_H^3 - v^2) + \sqrt{(1 - a^3 u_H^3 - v^2)^2 + 4a^3 u_H^3} \right). \quad (4.9)$$

Thus we obtain the drag force is

$$f = \frac{1}{2\pi\alpha'} \left( \frac{u_c}{R} \right)^{3/2} h(u_c)v. \quad (4.10)$$

In the figure 11, it shows this drag force how to depend on the non-commutative parameter  $b$ . At a fixed velocity  $v$ , the drag force will be decreased with increasing the value  $b$ . And

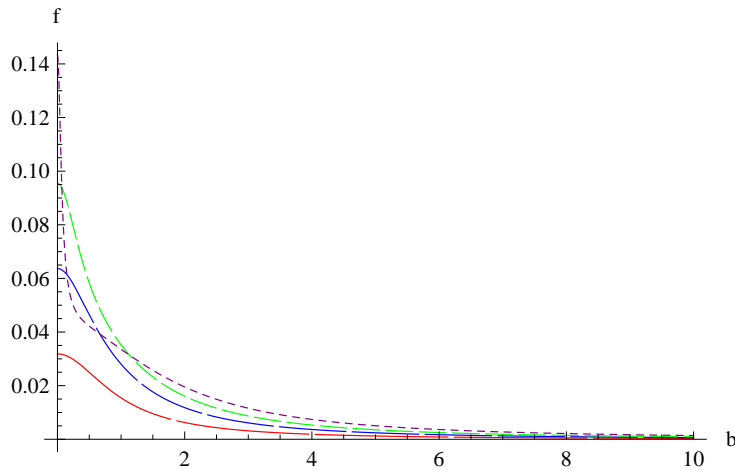


Figure 11: The drag force varies with the parameter  $b$  at  $v = 0.2, 0.4, 0.6, 0.9$  (red, blue, green and purple) or (the length of the dashed line segment is decreased). Here we already choose  $R = u_H = 1$  in plotting this figure.

at some large  $b$ , the drag force will vanish. Thus, the NS-NS  $B_{12}$  field can decrease the viscosity of the non-commutative QGP to a moving quark.

If the parameter  $a$  is very small, then the  $u_c$  can be expanded as

$$u_c^3 = \frac{u_H^3}{1-v^2} \left( 1 - \frac{v^2 u_H^3}{(1-v^2)^2} a^3 \right) + \mathcal{O}(a). \quad (4.11)$$

So at the leading order, the drag force becomes

$$f = \frac{1}{2\pi\alpha'} \left( \frac{u_H}{R} \right)^{3/2} \frac{v}{\sqrt{1-v^2}} \left( 1 - \frac{v^2 u_H^3}{(1-v^2)^2} a^3 \right). \quad (4.12)$$

And if let the non-commutative parameter  $a^3 = \frac{b^3}{R^3} = 0$ , this drag force reduces to the commutative case.

## 4.2 Meson in non-commutative QGP

Now we consider a meson moving through the non-commutative hot QGP. Here the black hole background is the metric (2.6). Defined  $\rho^2 = x_1^2 + x_2^2$ , then this gravity background is written as

$$ds^2 = \left( \frac{u}{R} \right)^{3/2} [-Hdt^2 + h(d\rho^2 + \rho^2 d\varphi^2) + dx_3^2 + dx_4^2] + \left( \frac{R}{u} \right)^{3/2} H^{-1} du^2, \\ B_{\rho\varphi} = B_{12}\rho. \quad (4.13)$$

where the  $S^4$  part is omitted. To study a meson moving through the QGP with a velocity  $v$ , we instead to choose the meson to be rest, while boost a QGP wind along the direction  $x_3$  with a constant velocity  $v$  [29] and [30]. Then the final metric takes the following form

$$ds^2 = -Adt^2 + 2Bdtdx_3 + Cdx_3^2 + g_{xx}h(d\rho^2 + \rho^2 d\varphi^2) + g_{uu}du^2, \quad (4.14)$$

where we have defined

$$g_{xx} = \left( \frac{u}{R} \right)^{3/2}, \quad H = 1 - K, \quad g_{uu} = \left( \frac{R}{u} \right)^{3/2} H^{-1}, \\ A = g_{xx}(1 - K \cosh^2 \eta), \quad B = g_{xx}K \sinh \eta \cosh \eta, \quad C = g_{xx}(1 + K \sinh^2 \eta), \quad (4.15) \\ \sinh \eta = \gamma v, \quad \cosh \eta = \gamma, \quad \gamma = 1/\sqrt{1-v^2}.$$

Now we study the open string in the background (4.14) and (4.15). Here we focus on the chiral symmetry breaking phase at high temperature. The two endpoints of this open

string attach on the connected D8- $\overline{\text{D8}}$  flavor brane. Then the worldsheet coordinates of the open spinning string can be parameterized as follows

$$\tau = t, \quad \sigma = \rho, \quad \varphi = \omega t, \quad x_3(\sigma), \quad u(\sigma). \quad (4.16)$$

If we set the dipole distance of  $q\bar{q}$  pair in the boundary is  $L$ , and the dipole is relative to the direction  $x_3$  at an angle  $\theta \in [0, \pi/2]$  in the  $(\rho, x_3)$  plane, then the  $\sigma$  is chosen in the range  $-\frac{L}{2} \sin \theta \leq \sigma \leq \frac{L}{2} \sin \theta$ . And the boundary conditions for  $x_3(\rho)$  is taken as  $x_3(\pm \frac{L}{2} \sin \theta) = \pm \frac{L}{2} \cos \theta$ . For the variable  $u(\rho)$ , its boundary value satisfies  $u(\pm \frac{L}{2} \sin \theta) \rightarrow \infty$ . Thus, the dynamics of open spinning string can be described by the Nambu-Goto action

$$S_{NG} = -\frac{1}{2\pi\alpha'} \int d\tau d\sigma \sqrt{-\det g_{\alpha\beta}} + \frac{1}{2\pi\alpha'} \int P[B] \quad (4.17)$$

with the induced metric  $g_{\alpha\beta} = G_{\mu\nu} \partial_\alpha x^\mu \partial_\beta x^\nu$  on the string worldsheet

$$g_{\tau\tau} = -A + g_{xx} h \rho^2 \omega^2, \quad g_{\tau\sigma} = B x'_3, \quad g_{\sigma\sigma} = g_{xx} h + C x_3'^2 + g_{uu} u'^2. \quad (4.18)$$

Its determinant and the pullback of the NS-NS  $B_{12}$  field are

$$\begin{aligned} -g_1 &\equiv -\det g_{\alpha\beta} = g_{xx}(1 - K \cosh^2 \eta - h\rho^2\omega^2)(g_{xx}h + g_{uu}u'^2) + \\ &\quad g_{xx}^2[1 - K - (1 + K \sinh^2 \eta)h\rho^2\omega^2]x_3'^2, \\ P[B] &= B_{12}\rho\omega d\sigma d\tau, \end{aligned} \quad (4.19)$$

where the sign ' in the formula denotes  $\partial_\sigma$ . From the formulas (4.17) and (4.19), the equations of motion for the variables  $x_3$  and  $u$  read

$$p = \frac{g_{xx}^2[1 - K - (1 + K \sinh^2 \eta)h\rho^2\omega^2]}{\sqrt{-g_1}} x_3' \quad (4.20)$$

$$\partial_u(\sqrt{-g_1} - B_{12}\rho\omega) = \partial_\sigma \left( \frac{g_{xx}g_{uu}(1 - K \cosh^2 \eta - h\rho^2\omega^2)u'}{\sqrt{-g_1}} \right) \quad (4.21)$$

where  $p$  is a integral constant. Since the Lagrangian explicitly depends on the variable  $\sigma$ , it means that the Hamiltonian is not conserved with respect to the variable  $\sigma$ . Also the equation (4.21) explicitly depends on the variable  $\sigma$ , the equations (4.20) and (4.21) are difficult to analytically solve. If the angular velocity  $\omega$  is equal to zero, then the pullback of the NS-NS  $B_{12}$  field and the determinant of the induced metric (4.19) don't explicitly depend on this variable. In this case, there exists two conserved charges. One is the Hamiltonian relative to the variable  $\sigma$ , the other is the  $p$  in the equation (4.20). Such meson  $q\bar{q}$  in QGP has been extensively studied in [29]-[32]. And there are not drag force

to the meson moving through the QGP by the arguments [28] and [31]. From equation (4.21), if  $\omega = 0$ , then it is explicitly symmetric under the transformation  $\sigma \leftrightarrow -\sigma$ . The  $u'(\sigma)$  decreases in the range  $-\frac{L}{2} \sin \theta < \sigma < 0$ , and is equal to zero at the critical point  $\sigma = 0$ , then increases to infinity in the range  $0 < \sigma < \frac{L}{2} \sin \theta$ .

For simplicity, we mainly consider the case:  $x'_3 = 0$ ,  $\sin \theta = 1$ ,  $v = 0$  and a constant angular velocity  $\omega$  in the following. It means the dipole is vertical with the coordinate  $x_3$ , and the shape of string is independent to the coordinate  $x_3$ . So the determinant of the induced metric on string worldsheet becomes

$$-g_2 = -\det g_{\alpha\beta} = g_{xx}(H - h\rho^2\omega^2)(g_{xx}h + g_{uu}u'^2). \quad (4.22)$$

Since it must be non-negative, which implies there exists a constraint  $1 \geq K + h\rho^2\omega^2$ . Thus, for a given angular velocity  $\omega$ , the variable  $u(\rho)$  has a bound. We explicitly show this bound in the figure 12. The string shape must be located above the corresponding

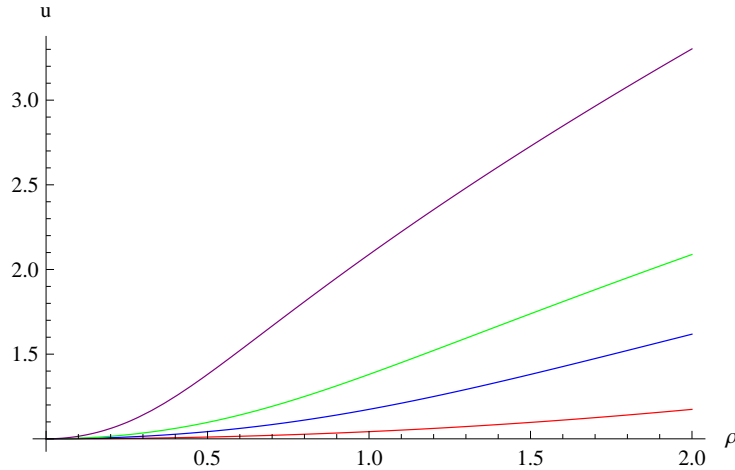


Figure 12: This figure shows the bound for the  $u(\rho)$  at  $\omega = 0.5, 1, 1.5, 3$  (red, blue, green and purple (from bottom to top)). We choose the  $u_H = R = 1$ .

curve for a fixed value  $\omega$ .

Now the equations of motions (4.20) and (4.21) become

$$p = 0$$

$$\partial_u(\sqrt{-g_2} - B_{12}\rho\omega) = \partial_\sigma \left( \frac{(H - h\rho^2\omega^2)u'}{H\sqrt{-g_2}} \right). \quad (4.23)$$

Then we get the shape of this rotating string shown in the figure 13 and 14. Here we only plot the zero node (the times of crossing the  $u$  coordinate) solution and already set

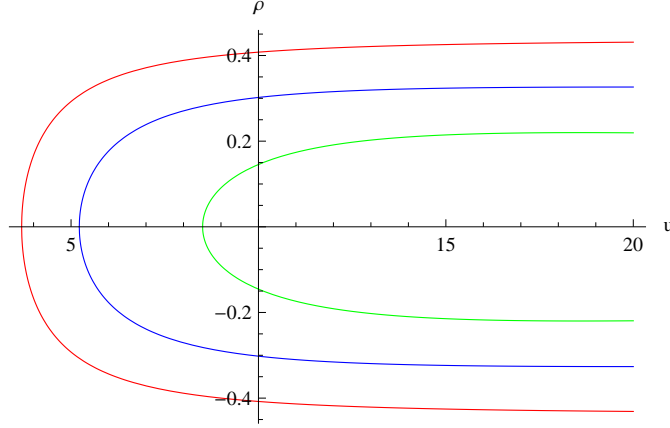


Figure 13: It is the string shape with  $\omega = 1, 1.5, 3$  (red, blue and green) or (from left to right) and  $b = 0$ .

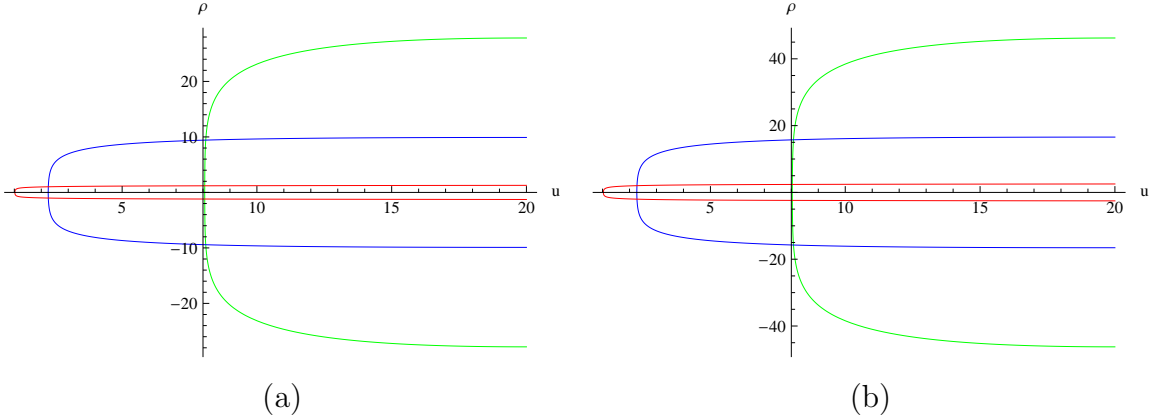


Figure 14: The shape of string is shown: (a) at  $\omega = 1, 1.5, 3$  (red, blue, green) or (from left to right) and  $b = 3$ ; (b) at  $\omega = 1, 1.5, 3$  (red, blue, green) or (from left to right) and  $b = 5$ .

$R = u_H = 1$ . With increasing the angular velocity  $\omega$  at  $b = 0$ , the distance between quark and anti-quark is became smaller, and the lowest point of this string is increased. But at a finite  $b$ , the separation of quark and anti-quark is increased with increasing the angular velocity  $\omega$ . At a fixed  $\omega$ , the lowest point of this spinning sting is became smaller with increasing the non-commutative parameter  $b$ .

With the equation (4.17) and (4.22), we obtain the energy and the angular momentum for this spinning open string. The string energy is

$$E = \frac{1}{\pi\alpha'} \int_0^{\frac{L}{2}} d\sigma \frac{g_{xx}^2}{\sqrt{-g_2}} \left( (1 - K) \left( h + \frac{g_{uu}}{g_{xx}} u'^2 \right) \right). \quad (4.24)$$

If subtracting the self-energy of the isolated quark and anti-quark, one can get the finite

bound energy of the  $q\bar{q}$ . And angular momentum is derived as

$$J = \frac{1}{\pi\alpha'} \int_0^{\frac{l}{2}} d\sigma \frac{\omega \rho^2 g_{xx}^2 h}{\sqrt{-g_2}} \left( h + \frac{g_{uu}}{g_{xx}} u'^2 \right) - \frac{1}{\pi\alpha'} \int_0^{\frac{l}{2}} d\sigma B_{12} \rho. \quad (4.25)$$

It corresponds to the spin of a meson  $q\bar{q}$  in the boundary theory. Using the equations (4.24) and (4.25), the Regge trajectory i.e. the relations between  $E^2$  and  $J$ , can be derived.

Now we investigate the relations  $E^2(\omega)$ ,  $J(\omega)$  and  $E^2(J)$ . Firstly, we consider the  $b = 0$  case, and plot the figures 15 and 16 in below<sup>5</sup>. The energy square  $E^2$  and the angular momentum  $J$  have a maximum value at a special angular velocity value  $w$ . The function  $E^2(J)$  has two branches relative to the angular momentum  $J$ . With increasing the angular momentum (increasing the angular velocity), the  $E^2$  is increased. After a maximum value, the value  $E^2$  is decreased with decreasing the angular momentum  $J$  (but increasing the angular velocity). Since our model reduces to the Sakai-Sugimoto model at the case  $b = 0$ , these results here is same as in [25] and [28].

Then we consider a finite non-commutative parameter  $b$  at finite temperature. The figures 17 and 18 are plotted. Explicitly, the curves in figures still have these properties as in 15 and 16. However, because of the effects of the NS-NS  $B_{12}$  field, the curves become more smoothly. With increasing the parameter  $b$ , the energy square  $E^2$  almost isn't changed, but the angular momentum  $J$  is increased.

If the temperature vanishes, i.e.  $u_H = 0$ , and  $b$  is a finite value, then the behaviors of the  $E^2(\omega)$ ,  $J(\omega)$  and  $E^2(J)$  are shown in the figures 19 and 20. These results are very similar to the finite temperature cases. And if let the temperature and parameter to vanish together, then such results are already investigated in [25] and [28]. From the figures 15-20, it is clear when the angular velocity  $\omega$  is equal to zero, then the angular momentum  $J$  vanishes.

If chosen the angle between the dipole and  $x_3$  is  $\theta = 0$ , then the wind is parallel to the  $q\bar{q}$  dipole. Now the worldsheet coordinates parameterization (4.16) is not well defined. Instead, the string worldsheet gauge is chosen as

$$\tau = t, \quad \sigma = x_3, \quad \varphi = \omega t, \quad u(\sigma), \quad \rho(\sigma). \quad (4.26)$$

Then the induced metric, its determinant and the pullback of NS-NS  $B_{12}$  field are listed as

$$\begin{aligned} g_{\tau\tau} &= -A + g_{xx} h \rho^2 \omega^2, \quad g_{\tau\rho} = B, \quad g_{\sigma\sigma} = C + g_{xx} h \rho'^2 + g_{uu} u'^2, \\ -g_3 &= g_{xx}^2 (1 - K - (1 + K \sinh^2 \eta) h \rho^2 \omega^2 \end{aligned}$$

---

<sup>5</sup> we set  $R = u_H = 1$  and  $u_\infty = 20$  in the figures 15-20

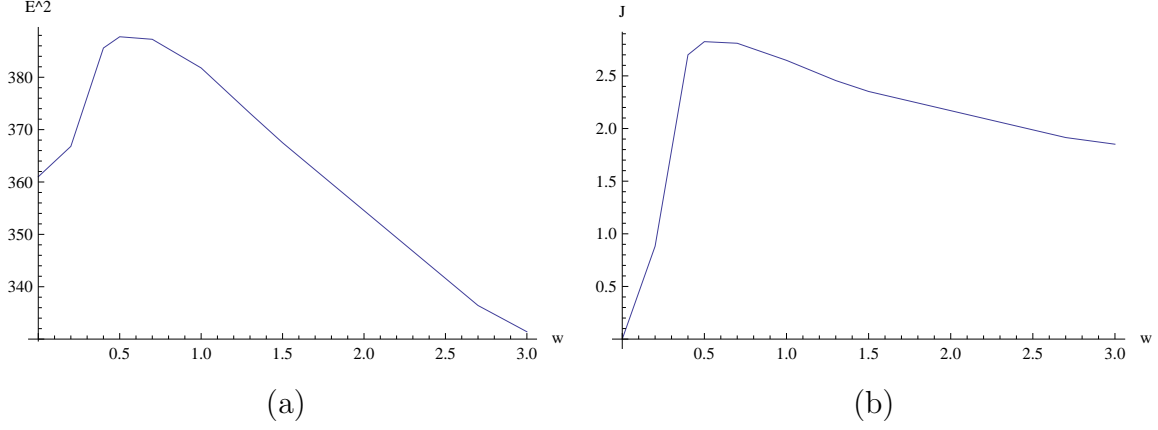


Figure 15: (a)  $E^2$  varies with the angular velocity  $\omega$  at  $b = 0$ ; (b) The angular momentum  $J$  varies with  $\omega$  at  $b = 0$ .

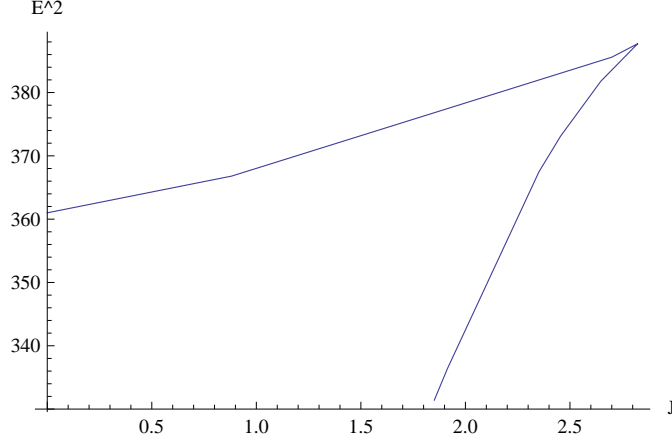


Figure 16: It is the Regge behavior  $E^2(J)$  vs  $J$  at  $b = 0$ .

$$P[B]_{\tau\sigma} = B_{12}\rho\rho'\omega. \quad (4.27)$$

$$+ (1 - K \cosh^2 \eta - h\rho^2\omega^2) \left( h\rho'^2 + \frac{g_{uu}}{g_{xx}} u'^2 \right),$$

Since the Lagrangian does not explicitly depend on the variable  $\sigma$ , the Hamiltonian is conserved with respect to the variable  $\sigma$ . Then the conserved constant  $q$  is defined as

$$q = \frac{g_{xx}^2 [1 - K - (1 + K \sinh^2 \eta) \rho^2 \omega^2]}{\sqrt{-g_3}}. \quad (4.28)$$

And the other equations of motion are

$$\partial_\sigma \left( \frac{g_{xx}^2 (1 - K \cosh^2 \eta - h\rho^2\omega^2) h\rho'}{\sqrt{-g_3}} - B_{12}\rho\omega \right) =$$

$$\frac{\rho g_{xx}^2 h\omega^2 (1 + K \sinh^2 \eta + h\rho'^2 + \frac{g_{uu}}{g_{xx}} u'^2)}{\sqrt{-g_3}} - B_{12}\omega\rho',$$

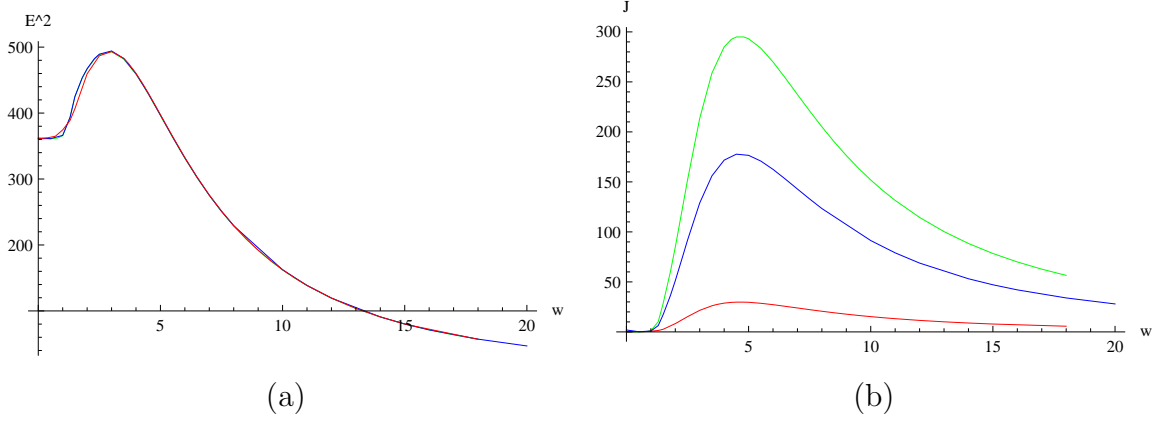


Figure 17: (a)  $E^2$  varies with  $\omega$  at  $b = 0.5, 3, 5$  (red, blue, green). The curved lines  $E^2(\omega)$  is almost same at different constant value  $b$ ; (b) It is shown the relation between  $J$  and  $\omega$  at  $b = 0.5, 3, 5$  (red, blue, green) or (from bottom to top).

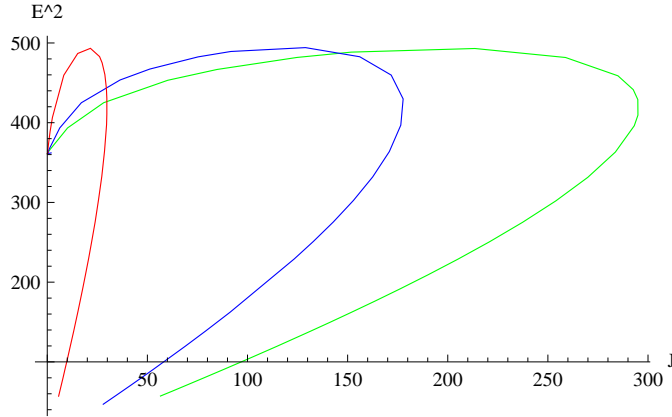


Figure 18:  $E^2$  varies with the angular momentum  $J$  at  $b = 0.5, 3, 5$  (red, blue, green) or (from left to right).

$$\partial_u(\sqrt{-g_3} - B_{12}\omega\rho\rho') = \partial_\sigma \left( \frac{g_{xx}g_{uu}(1 - K \cosh^2 \eta - h\rho^2\omega^2)u'}{\sqrt{-g_3}} \right). \quad (4.29)$$

One can use the equation (4.28) and the equations of motion (4.29) to calculate the dynamics of a open string in the gravity background (2.6). In addition, the energy and angular momentum of open spinning string at the  $\theta = 0$  case are

$$E = \frac{1}{\pi\alpha'} \int_0^{\frac{L}{2}} d\sigma \frac{g_{xx}^2 \left( 1 - K + (1 - K \cosh^2 \eta)(h\rho'^2 + \frac{g_{uu}}{g_{xx}}u'^2) \right)}{\sqrt{-g_3}},$$

$$J = \frac{1}{\pi\alpha'} \int_0^{\frac{L}{2}} d\sigma \frac{\omega\rho^2 g_{xx}^2 h \left( 1 + K \sinh^2 \eta + h\rho'^2 + \frac{g_{uu}}{g_{xx}}u'^2 \right)}{\sqrt{-g_3}}$$

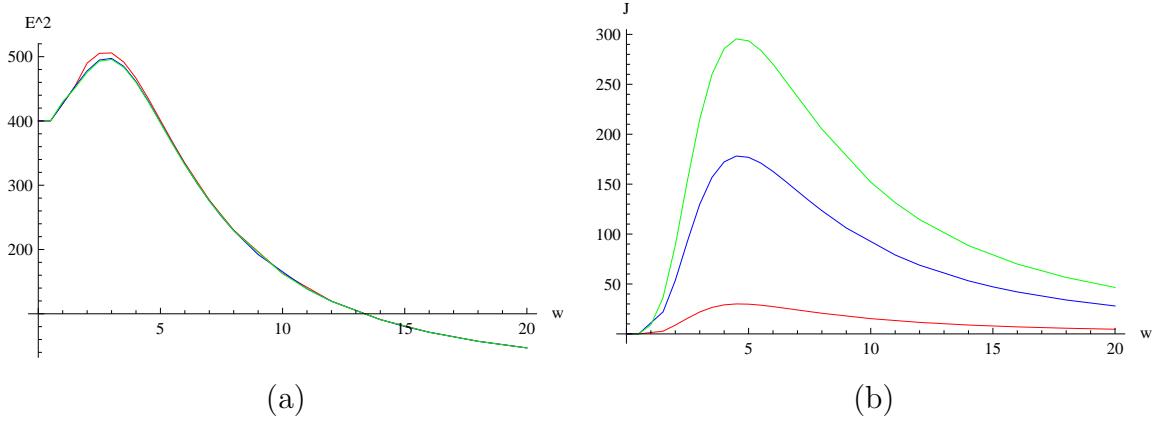


Figure 19: (a)  $E^2$  varies with  $\omega$  at  $b = 0.5, 3, 5$  (red, blue, green) and  $T = 0$ . These three curves are almost overlapped each other; (b)  $J$  varies with  $\omega$  at  $b = 0.5, 3, 5$  (red, blue, green) or (from bottom to top) and  $T = 0$ .

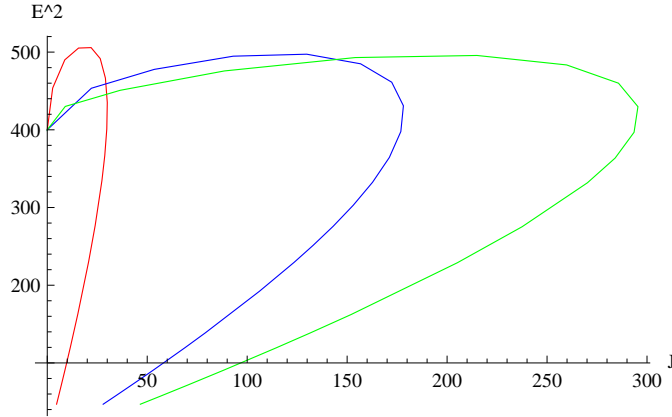


Figure 20: This is the figure about  $E^2$  varying with  $J$  at  $b = 0.5, 3, 5$  (red, blue, green) or (from left to right) and  $T = 0$ .

$$-\frac{1}{\pi\alpha'} \int_0^{\frac{L}{2}} d\sigma B_{12}\rho\rho'. \quad (4.30)$$

If the coordinate  $\rho$  is constant, and  $\omega = 0$ , then it reduces to the similar case studied in [29]-[32]. Otherwise, if  $v = 0$ , then the metric determinant and the equations (4.28), (4.29) and (4.30) reduce to

$$\begin{aligned} -g_4 &= g_{xx}^2(1 - K - h\rho^2\omega^2)(1 + h\rho'^2 + \frac{g_{uu}}{g_{xx}}u'^2), \\ q &= \frac{g_{xx}^2(1 - K - h\rho^2\omega^2)}{\sqrt{-g_4}}, \\ \partial_\sigma \left( \frac{g_{xx}^2 h(1 - K - h\rho^2\omega^2)\rho'}{\sqrt{-g_4}} - B_{12}\rho\omega \right) &= \end{aligned}$$

$$\begin{aligned}
& \frac{\rho g_{xx}^2 h \omega^2 (1 + h \rho'^2 + \frac{g_{uu}}{g_{xx}} u'^2)}{\sqrt{-g}} - B_{12} \omega \rho', \\
\partial_u (\sqrt{-g_4} - B_{12} \omega \rho \rho') &= \partial_\sigma \left( \frac{g_{xx} g_{uu} (1 - K - h \rho^2 \omega^2) u'}{\sqrt{-g_4}} \right), \\
E &= \frac{1}{\pi \alpha'} \int_0^{\frac{L}{2}} d\sigma \frac{g_{xx}^2 (1 - K) (1 + h \rho'^2 + \frac{g_{uu}}{g_{xx}} u'^2)}{\sqrt{-g_4}}, \\
J &= \frac{1}{\pi \alpha'} \int_0^{\frac{L}{2}} d\sigma \frac{\omega \rho^2 g_{xx}^2 h (1 + h \rho'^2 + \frac{g_{uu}}{g_{xx}} u'^2)}{\sqrt{-g_4}} - \frac{1}{\pi \alpha'} \int_0^{\frac{L}{2}} d\sigma B_{12} \rho \rho'.
\end{aligned} \tag{4.31}$$

One can discuss the relations of the energy  $E$ , angular momentum  $J$  with the angular velocity  $\omega$ , and investigate the Regge trajectory behavior  $E^2(J)$ . Here we only list these equations, the numerical calculations can be done by using the same method as before.

## 5 Summaries

In this paper, we construct a holographic model by the D4-D8/ $\overline{\text{D8}}$  brane configuration with a NS-NS  $B_{12}$  field. The effective theory on the intersecting region of this brane configuration is a four-dimensional non-commutative field theory. In the strong coupling regime, we investigate some underlying low energy dynamics of this theory by using the supergravity/Born-Infeld approximation.

If don't turn on the gauge field on the flavor D8-brane, we find the effective D8-brane action is similar to the commutative case [12] except for some coefficients. So all the dynamics, for example the chiral symmetry breaking, are same. However, with a magnetic field along the direction  $x_1$  and  $x_2$ , then the DBI action of the flavor D8-brane includes the non-commutative parameter  $b$  and magnetic field parameter  $B$ . We analyze their influences on the asymptotic distance  $L$  between D8 and  $\overline{\text{D8}}$  brane and the energy difference  $\delta S$  of two solutions. In both the low temperature and high temperature phase, the distance  $L$  is increased with increasing the magnetic parameter at a fixed value  $b$ . However, the thing is conversed if increasing the non-commutative parameter  $b$  at a fixed value  $B$ . It means the parameter  $B$  and  $b$  have converse contributions to the asymptotic distance  $L$ . For the energy difference, it is always negative with arbitrary value  $B$  and  $b$  at low temperature. So the chiral symmetry is independent on the magnetic field and non-commutative parameter. And it is always broken. In the high temperature phase, the energy difference  $\delta S$  between the connected and separated solutions has a critical temperature  $T_\chi$ . At  $b = 0$ , our model reduces to the Sakai-Sugimoto model with a

magnetic field, and here the results is same as in [24]. At a finite fixed value  $b$ , the critical point  $y_H$  becomes smaller with increasing  $B$ . However, it become larger with increasing  $b$  at a fixed  $B$ . As similar as the distance  $L$ , the contributions of the  $B$  and  $b$  are also conversed. This may be understood from the equation (2.16), in which the parameter  $B$  is proportional to  $1/b$ . Below the critical points, the energy difference  $\delta S$  is negative. Then the connected D8- $\overline{\text{D8}}$  brane solution is dominated, the chiral symmetry is broken  $U(N_f) \times U(N_f) \rightarrow U(N_f)_{\text{diag}}$ . Otherwise,  $\delta S$  is positive, and the dominated solution is the separated D8- $\overline{\text{D8}}$  configuration, and the chiral symmetry will be restored. Thus there exists a first order chiral phase transition at these critical points.

We also generalize to consider some other branes configurations. Some three- and four-dimensional non-commutative field theories are constructed through some intersecting brane configurations. The results is similar to the cases of D8- $\overline{\text{D8}}$  brane configurations. Maybe these models have some applications to study the condensed matter physics or something else.

And we investigated the dynamics of a fundamental string in the high temperature background (2.6). We find the non-commutative parameter will decrease the drag force. The relations  $E^2(\omega)$ ,  $J(\omega)$  and  $E^2(J)$  become more smoothly than the results without the non-commutative effects. With increasing the parameter  $b$ , the energy  $E^2$  is almost unchanged, and the angular momentum  $J$  is became larger.

There are some generalizations to this holographic model. The first one is to study the meson spectra through investigating the world-volume field fluctuations on the flavor brane. The fluctuation DBI action is similar to the commutative case just like in [13], however, the Chern-simons term contains some non-commutative contributions. Then one can investigate the Nambu-Goldstone bosons corresponding to the chiral symmetry breaking in the meson spectra. The second is to consider a chemical potential in this and other general holographic models by using the method in [33]. Also one can calculate the shear and bulk viscosity of non-commutative QGP as the similar way in [34]. Finally, following in [35], to construct the baryons in this holographic model is also interesting.

## Acknowledgments

Wei-shui thank CQUeST for providing an office. It is more convenient for me to study and research. This work of Yunseok was supported by the Korea Science and Engineering Foundation (KOSEF) grant funded by the Korea government(MEST) through the Center

for Quantum Spacetime(CQeST) of Sogang University with grant number R11-2005-021. This work of SJS and Weishui is supported by KOSEF Grant R01-2007-000-10214-0 and also by the SRC Program of the KOSEF through the Center for Quantum SpaceTime (CQeST) of Sogang University with grant number R11-2005-021.

## A D-brane backgrounds with a NS-NS field

In this appendix, we give the gravity backgrounds used in the main part of this paper.

Turning on a constant NS-NS  $B_{MN}$  background field in a flat spacetime, the open string in this background can be quantized. Then, due to this  $B_{MN}$  field, the field theory on the D-brane worldvolume is non-commutative [16]. The non-commutative parameter is proportional to this constant NS-NS  $B_{MN}$  field.

The gravity solution of D-brane with a NS-NS  $B_{MN}$  field was constructed in [17]-[19]. In the following, we mainly focus on the D4-brane backgrounds with a NS-NS  $B_{MN}$  background field. This supergravity solution is

$$\begin{aligned}
ds^2 &= f^{-1/2} [-dt^2 + h(dx_1^2 + dx_2^2) + dx_3^2 + dx_4^2] + f^{1/2}(dr^2 + r^2 d\Omega_4^2), \\
f &= 1 + \frac{\alpha' R^3}{r^3}, \quad R^3 = \frac{\pi^2 g_{\text{YM}}^2 N_c}{4 \cos \theta}, \\
h^{-1} &= \sin^2 \theta f^{-1} + \cos^2 \theta, \\
B_{12} &= h f^{-1} \tan \theta, \quad e^{2\phi} = g_s^2 f^{-1/2} h, \\
C_{01234} &= g_s^{-1} (1 - f^{-1}) h \cos \theta, \quad C_{034} = g_s^{-1} (1 - f^{-1}) \sin \theta.
\end{aligned} \tag{A.1}$$

where  $g_{\text{YM}}^2 = (2\pi)^2 g_s l_s$ . Actually, it is a bound state of the D2 and D4 brane [17]. The D2-brane extends along the  $t$ ,  $x_3$  and  $x_4$  directions, and D4-brane's worldvolume coordinates are  $t$  and  $x_{1,\dots,4}$ . This solution can be got by applying the delocalization and rotation on a D3-brane and doing T-duality. The NS-NS  $B_{12}$  field is produced through the T-duality acting on the non-trivial gravity background.

Define some parameters as

$$u = r/\alpha', \quad g'_s = \frac{g_s b}{l_s}, \quad b = \alpha' \tan \theta, \quad x'_{1,2} = \frac{b}{\alpha'} x_{1,2}. \tag{A.2}$$

If choose the limit  $\alpha' \rightarrow 0$ , and let the above parameters to be fixed, then the gravity solution (A.1) becomes<sup>6</sup>

$$ds^2 = \left( \frac{\alpha'^2 u^3}{R^3} \right)^{1/2} [-dt^2 + h(dx_1'^2 + dx_2'^2) + dx_3^2 + dx_4^2] + \left( \frac{R^3}{\alpha'^2 u^3} \right)^{1/2} (du^2 + u^2 d\Omega_4^2),$$

---

<sup>6</sup>We already replace the  $g'_s, x'_{1,2}$  by  $g_s, x_{1,2}$ , and will set  $\alpha' = 1$  in the main part of this paper.

$$\begin{aligned}
R^3 &= \pi^4 g'_s N_c, \quad h = \frac{1}{1 + a^3 u^3}, \quad a^3 \equiv \frac{b^2}{R^3}, \\
B_{12} &= \frac{\alpha' a^3 u^3}{b(1 + a^3 u^3)} = \frac{\alpha'}{b}(1 - h), \quad e^{2\phi} = g_s'^2 \frac{\alpha'^2}{R^{3/2} b^2} u^{3/2} h, \\
C_{01234} &= g_s'^{-1} \alpha'^{1/2} h, \quad C_{034} = g_s'^{-1} \alpha'^{-1/2} b.
\end{aligned} \tag{A.3}$$

The gravity theory on this near horizon background is dual to a five-dimensional non-commutative field theory. Here the coordinates  $x_1$  and  $x_2$  in the boundary theory is non-commutative,  $[x_1, x_2] \sim b$ . One can generalize to consider some other bound states. For example, if consider the D4-D2-D2-D0 case, then one find the space coordinate  $x_3$  and  $x_4$  of the boundary field theory will be non-commutative [17] and [19].

From the solution (A.3), the curvature scalar is

$$\mathcal{R} \sim \frac{1}{g_{eff}}, \quad g_{eff} \sim g_s N_c u. \tag{A.4}$$

And the effective string coupling constant is

$$e^\phi \sim \frac{g_{eff}^{3/2}}{N_c \sqrt{1 + a_{eff}^3}}, \quad a_{eff} \sim \left( \frac{bu^2}{g_{eff}} \right)^{2/3}, \tag{A.5}$$

where  $a_{eff}$  is an effective non-commutative parameter. if  $a_{eff} \ll 1$ , then it means the non-commutative effect can be neglected, and the non-commutative field theory will reduce to a commutative theory. when the following condition

$$\mathcal{R} \ll 1, \quad e^\phi \ll 1 \tag{A.6}$$

are satisfied, the low energy dynamics on the D-brane can be investigated by the supergravity approximation. More detail discussions can be found in [19].

A non-extremal generalization of the supergravity solution (A.1) is

$$\begin{aligned}
ds^2 &= f^{-1/2} [-H dt^2 + h(dx_1^2 + dx_2^2) + dx_3^2 + dx_4^2] + f^{1/2} (H^{-1} dr^2 + r^2 d\Omega_4^2), \\
H &= 1 - \frac{r_H^3}{r^3}, \quad R^3 = \frac{\pi^2 g_{YM}^2 N_c}{4 \cos \theta}, \\
h^{-1} &= \sin^2 \theta f^{-1} + \cos^2 \theta, \\
B_{12} &= h f^{-1} \tan \theta, \quad e^{2\phi} = g_s^2 f^{-1/2} h, \\
C_{01234} &= g_s^{-1} (1 - f^{-1}) h \cos \theta, \quad C_{034} = g_s^{-1} (1 - f^{-1}) \sin \theta.
\end{aligned} \tag{A.7}$$

Then, in the decoupling limit (A.2), the near horizon geometry of the metric (A.7) is

$$\begin{aligned}
ds^2 &= \left( \frac{u}{R} \right)^{3/2} [-H dt^2 + h(dx_1^2 + dx_2^2) + dx_3^2 + dx_4^2] + \left( \frac{R}{u} \right)^{3/2} (H^{-1} du^2 + u^2 d\Omega_4^2), \\
H &= 1 - \frac{u_H^3}{u^3}.
\end{aligned} \tag{A.8}$$

The other background fields are same as the solution (A.3). The corresponding effective theory in the boundary of the gravity background (A.8) is a finite temperature generalization to the zero temperature case of the gravity background (A.3).

## References

- [1] G. 't Hooft, “Dimensional reduction in quantum gravity,” arXiv:gr-qc/9310026; L. Susskind, “The World As A Hologram,” J. Math. Phys. **36**, 6377 (1995) [arXiv:hep-th/9409089].
- [2] J. M. Maldacena, “The large N limit of superconformal field theories and supergravity,” Adv. Theor. Math. Phys. **2**, 231 (1998) [Int. J. Theor. Phys. **38**, 1113 (1999)] [arXiv:hep-th/9711200].
- [3] S. S. Gubser, I. R. Klebanov and A. M. Polyakov, “Gauge theory correlators from non-critical string theory,” Phys. Lett. B **428**, 105 (1998) [arXiv:hep-th/9802109].
- [4] E. Witten, “Anti-de Sitter space and holography,” Adv. Theor. Math. Phys. **2**, 253 (1998) [arXiv:hep-th/9802150].
- [5] O. Aharony, S. S. Gubser, J. M. Maldacena, H. Ooguri and Y. Oz, “Large N field theories, string theory and gravity,” Phys. Rept. **323**, 183 (2000) [arXiv:hep-th/9905111].
- [6] E. Witten, “Anti-de Sitter space, thermal phase transition, and confinement in gauge theories,” Adv. Theor. Math. Phys. **2**, 505 (1998) [arXiv:hep-th/9803131].
- [7] J. Polchinski and M. J. Strassler, “The string dual of a confining four-dimensional gauge theory,” arXiv:hep-th/0003136; I. R. Klebanov and M. J. Strassler, “Supergravity and a confining gauge theory: Duality cascades and chiSB-resolution of naked singularities,” JHEP **0008**, 052 (2000) [arXiv:hep-th/0007191]; J. M. Maldacena and C. Nunez, “Towards the large N limit of pure N = 1 super Yang Mills,” Phys. Rev. Lett. **86**, 588 (2001) [arXiv:hep-th/0008001].
- [8] A. Karch and E. Katz, “Adding flavor to AdS/CFT,” JHEP **0206**, 043 (2002) [arXiv:hep-th/0205236].

- [9] M. Kruczenski, D. Mateos, R. C. Myers and D. J. Winters, “Meson spectroscopy in AdS/CFT with flavour,” *JHEP* **0307**, 049 (2003) [arXiv:hep-th/0304032].
- [10] J. Babington, J. Erdmenger, N. J. Evans, Z. Guralnik and I. Kirsch, “Chiral symmetry breaking and pions in non-supersymmetric gauge/gravity duals,” *Phys. Rev. D* **69**, 066007 (2004) [arXiv:hep-th/0306018].
- [11] M. Kruczenski, D. Mateos, R. C. Myers and D. J. Winters, “Towards a holographic dual of large- $N(c)$  QCD,” *JHEP* **0405**, 041 (2004) [arXiv:hep-th/0311270].
- [12] T. Sakai and S. Sugimoto, “Low energy hadron physics in holographic QCD,” *Prog. Theor. Phys.* **113**, 843 (2005) [arXiv:hep-th/0412141]; T. Sakai and S. Sugimoto, “More on a holographic dual of QCD,” *Prog. Theor. Phys.* **114**, 1083 (2005) [arXiv:hep-th/0507073].
- [13] D. Arean, A. Paredes and A. V. Ramallo, “Adding flavor to the gravity dual of non-commutative gauge theories,” *JHEP* **0508**, 017 (2005) [arXiv:hep-th/0505181].
- [14] E. Antonyan, J. A. Harvey, S. Jensen and D. Kutasov, “NJL and QCD from string theory,” arXiv:hep-th/0604017; E. Antonyan, J. A. Harvey and D. Kutasov, “The Gross-Neveu model from string theory,” *Nucl. Phys. B* **776**, 93 (2007) [arXiv:hep-th/0608149]; E. Antonyan, J. A. Harvey and D. Kutasov, “Chiral symmetry breaking from intersecting D-branes,” *Nucl. Phys. B* **784**, 1 (2007) [arXiv:hep-th/0608177]; Y. h. Gao, W. s. Xu and D. f. Zeng, “NGN, QCD(2) and chiral phase transition from string theory,” *JHEP* **0608**, 018 (2006) [arXiv:hep-th/0605138]; V. Mazu and J. Sonnenschein, “Non critical holographic models of the thermal phases of QCD,” *JHEP* **0806**, 091 (2008) [arXiv:0711.4273 [hep-th]]; S. Kuperstein and J. Sonnenschein, “A New Holographic Model of Chiral Symmetry Breaking,” *JHEP* **0809**, 012 (2008) [arXiv:0807.2897 [hep-th]]; B. A. Burrington and J. Sonnenschein, “Holographic Dual of QCD from Black D5 Branes,” arXiv:0903.0628 [hep-th].
- [15] B. A. Burrington, J. T. Liu, L. A. Pando Zayas and D. Vaman, “Holographic duals of flavored  $N = 1$  super Yang-Mills: Beyond the probe approximation,” *JHEP* **0502**, 022 (2005) [arXiv:hep-th/0406207]; R. Casero, C. Nunez and A. Paredes, “Towards the string dual of  $N = 1$  SQCD-like theories,” *Phys. Rev. D* **73**, 086005 (2006) [arXiv:hep-th/0602027]; F. Benini, F. Canoura, S. Cremonesi, C. Nunez and

- A. V. Ramallo, “Unquenched flavors in the Klebanov-Witten model,” *JHEP* **0702**, 090 (2007) [arXiv:hep-th/0612118]; F. Benini, F. Canoura, S. Cremonesi, C. Nunez and A. V. Ramallo, “Backreacting Flavors in the Klebanov-Strassler Background,” *JHEP* **0709**, 109 (2007) [arXiv:0706.1238 [hep-th]]; F. Canoura, P. Merlatti and A. V. Ramallo, “The supergravity dual of 3d supersymmetric gauge theories with unquenched flavors,” *JHEP* **0805**, 011 (2008) [arXiv:0803.1475 [hep-th]]; D. Arean, P. Merlatti, C. Nunez and A. V. Ramallo, “String duals of two-dimensional (4,4) supersymmetric gauge theories,” *JHEP* **0812**, 054 (2008) [arXiv:0810.1053 [hep-th]].
- [16] N. Seiberg and E. Witten, “String theory and noncommutative geometry,” *JHEP* **9909**, 032 (1999) [arXiv:hep-th/9908142].
- [17] J. C. Breckenridge, G. Michaud and R. C. Myers, “More D-brane bound states,” *Phys. Rev. D* **55**, 6438 (1997) [arXiv:hep-th/9611174].
- [18] J. M. Maldacena and J. G. Russo, “Large N limit of non-commutative gauge theories,” *JHEP* **9909**, 025 (1999) [arXiv:hep-th/9908134].
- [19] M. Alishahiha, Y. Oz and M. M. Sheikh-Jabbari, “Supergravity and large N non-commutative field theories,” *JHEP* **9911**, 007 (1999) [arXiv:hep-th/9909215].
- [20] N. Izhaki, J. M. Maldacena, J. Sonnenschein and S. Yankielowicz, “Supergravity and the large N limit of theories with sixteen supercharges,” *Phys. Rev. D* **58**, 046004 (1998) [arXiv:hep-th/9802042].
- [21] O. Aharony, J. Sonnenschein and S. Yankielowicz, “A holographic model of deconfinement and chiral symmetry restoration,” *Annals Phys.* **322**, 1420 (2007) [arXiv:hep-th/0604161]; A. Parnachev and D. A. Sahakyan, “Chiral phase transition from string theory,” *Phys. Rev. Lett.* **97**, 111601 (2006) [arXiv:hep-th/0604173].
- [22] V. G. Filev, C. V. Johnson, R. C. Rashkov and K. S. Viswanathan, “Flavoured large N gauge theory in an external magnetic field,” *JHEP* **0710**, 019 (2007) [arXiv:hep-th/0701001]; T. Albash, V. G. Filev, C. V. Johnson and A. Kundu, “Finite Temperature Large N Gauge Theory with Quarks in an External Magnetic Field,” *JHEP* **0807**, 080 (2008) [arXiv:0709.1547 [hep-th]]; T. Albash, V. G. Filev, C. V. Johnson and A. Kundu, “Quarks in an External Electric Field in Finite Temperature

- Large N Gauge Theory,” JHEP **0808**, 092 (2008) [arXiv:0709.1554 [hep-th]]; J. Erdmenger, R. Meyer and J. P. Shock, “AdS/CFT with Flavour in Electric and Magnetic Kalb-Ramond Fields,” JHEP **0712**, 091 (2007) [arXiv:0709.1551 [hep-th]]; A. V. Zayakin, “QCD Vacuum Properties in a Magnetic Field from AdS/CFT: Chiral Condensate and Goldstone Mass,” JHEP **0807**, 116 (2008) [arXiv:0807.2917 [hep-th]]; V. G. Filev, C. V. Johnson and J. P. Shock, “Universal Holographic Chiral Dynamics in an External Magnetic Field,” arXiv:0903.5345 [hep-th].
- [23] O. Bergman, G. Lifschytz and M. Lippert, “Response of Holographic QCD to Electric and Magnetic Fields,” JHEP **0805**, 007 (2008) [arXiv:0802.3720 [hep-th]].
- [24] C. V. Johnson and A. Kundu, “External Fields and Chiral Symmetry Breaking in the Sakai-Sugimoto Model,” JHEP **0812**, 053 (2008) [arXiv:0803.0038 [hep-th]].
- [25] C. V. Johnson and A. Kundu, “Meson Spectra and Magnetic Fields in the Sakai-Sugimoto Model,” arXiv:0904.4320 [hep-th];
- [26] S. S. Gubser, “Drag force in AdS/CFT,” Phys. Rev. D **74**, 126005 (2006) [arXiv:hep-th/0605182].
- [27] T. Matsuo, D. Tomino and W. Y. Wen, “Drag force in SYM plasma with B field from AdS/CFT,” JHEP **0610**, 055 (2006) [arXiv:hep-th/0607178].
- [28] K. Peeters, J. Sonnenschein and M. Zamaklar, “Holographic melting and related properties of mesons in a quark gluon plasma,” Phys. Rev. D **74**, 106008 (2006) [arXiv:hep-th/0606195].
- [29] H. Liu, K. Rajagopal and U. A. Wiedemann, “An AdS/CFT calculation of screening in a hot wind,” Phys. Rev. Lett. **98**, 182301 (2007) [arXiv:hep-ph/0607062].
- [30] H. Liu, K. Rajagopal and U. A. Wiedemann, “Wilson loops in heavy ion collisions and their calculation in AdS/CFT,” JHEP **0703**, 066 (2007) [arXiv:hep-ph/0612168].
- [31] M. Chernicoff, J. A. Garcia and A. Guijosa, “The energy of a moving quark-antiquark pair in an N = 4 SYM plasma,” JHEP **0609**, 068 (2006) [arXiv:hep-th/0607089].

- [32] E. Caceres, M. Natsuume and T. Okamura, “Screening length in plasma winds,” JHEP **0610**, 011 (2006) [arXiv:hep-th/0607233].
- [33] N. Horigome and Y. Tanii, JHEP **0701**, 072 (2007) [arXiv:hep-th/0608198]; S. Kobayashi, D. Mateos, S. Matsuura, R. C. Myers and R. M. Thomson, JHEP **0702**, 016 (2007) [arXiv:hep-th/0611099]; D. Mateos, S. Matsuura, R. C. Myers and R. M. Thomson, “Holographic phase transitions at finite chemical potential,” JHEP **0711**, 085 (2007) [arXiv:0709.1225 [hep-th]]; S. Matsuura, “On holographic phase transitions at finite chemical potential,” JHEP **0711**, 098 (2007) [arXiv:0711.0407 [hep-th]]; S. Nakamura, Y. Seo, S. J. Sin and K. P. Yogendran, “A new phase at finite quark density from AdS/CFT,” J. Korean Phys. Soc. **52**, 1734 (2008) [arXiv:hep-th/0611021]; S. Nakamura, Y. Seo, S. J. Sin and K. P. Yogendran, “Baryon-charge Chemical Potential in AdS/CFT,” Prog. Theor. Phys. **120**, 51 (2008) [arXiv:0708.2818 [hep-th]]; O. Bergman, G. Lifschytz and M. Lippert, “Holographic Nuclear Physics,” JHEP **0711**, 056 (2007) [arXiv:0708.0326 [hep-th]]; A. Parnachev, “Holographic QCD with Isospin Chemical Potential,” JHEP **0802**, 062 (2008) [arXiv:0708.3170 [hep-th]].
- [34] K. Landsteiner and J. Mas, “The shear viscosity of the non-commutative plasma,” JHEP **0707**, 088 (2007) [arXiv:0706.0411 [hep-th]].
- [35] H. Hata, T. Sakai, S. Sugimoto and S. Yamato, “Baryons from instantons in holographic QCD,” arXiv:hep-th/0701280; D. K. Hong, M. Rho, H. U. Yee and P. Yi, “Chiral dynamics of baryons from string theory,” Phys. Rev. D **76**, 061901 (2007) [arXiv:hep-th/0701276].
- [36] L. Susskind, “The quantum Hall fluid and non-commutative Chern Simons theory,” arXiv:hep-th/0101029.